Static behaviour of functionally graded sandwich beams using a quasi-3D theory

Thuc P. Vo[a,*], Huu-Tai Thai[b], Trung-Kien Nguyen[c], Fawad Inam[a], Jaehong Lee[d]

[a] *Faculty of Engineering and Environment, Northumbria University, Newcastle upon Tyne, NE1 8ST, UK.*
[b] *School of Civil and Environmental Engineering, The University of New South Wales, NSW 2052, Australia.*
[c] *Faculty of Civil Engineering and Applied Mechanics, University of Technical Education Ho Chi Minh City, 1 Vo Van Ngan Street, Thu Duc District, Ho Chi Minh City, Vietnam*
[d] *Department of Architectural Engineering, Sejong University 98 Kunja Dong, Kwangjin Ku, Seoul 143-747, Korea.*

Abstract

This paper presents static behaviour of functionally graded (FG) sandwich beams by using a quasi-3D theory, which includes both shear deformation and thickness stretching effects. Various symmetric and non-symmetric sandwich beams with FG material in the core or skins under the uniformly distributed load are considered. Finite element model (FEM) and Navier solutions are developed to determine the displacement and stresses of FG sandwich beams for various power-law index, skin-core-skin thickness ratios and boundary conditions. Numerical results are compared with those predicted by other theories to show the effects of shear deformation and thickness stretching on displacement and stresses.

Keywords: A. Hybrid; C. Numerical analysis

1. Introduction

In recent years, there is a rapid increase in the use of functionally graded (FG) sandwich structures in aerospace, marine and civil engineering due to high strength-to-weight ratio. Since the shear deformation effects are more pronounced in these structures, the first-order shear deformation theory and higher-order shear deformation theories should be used. By using these theories, although many papers have been devoted to study static, vibration and buckling analysis of FG structures such as shells ([1]-[3]), plates ([4]-[8]), sandwich plates ([9]-[11]) and beams ([12]-[26]), only some of them are cited here. It should be noted that in these theories the thickness-stretching effect is ignored, which is especially significant for thick FG plates [27]. A quasi-3D theory, which includes both shear deformation and thickness stretching effects, assumes that the in-plane and out-plane displacements

*Corresponding author, tel.: +44 191 243 7856
Email address: thuc.vo@northumbria.ac.uk (Thuc P. Vo)

are a higher-order variation through the thickness. By using this theory, although many researchers studied bending analysis of FG plates ([28]-[40]) and FG sandwich ones ([41], [42]), as far as authors are aware, there is no work available for bending analysis of FG sandwich beams. As a result, a quasi-3D theory for this complicated problem is necessary, which is also the main purpose of this paper.

This work aims to study static behaviour of FG sandwich beams using a quasi-3D theory. The axial and transverse displacements are assumed to be cubic and parabolic variation through the thickness. FEM and Navier solutions are developed to determine the displacement and stresses of FG sandwich beams for various power-law index, skin-core-skin thickness ratios and boundary conditions. Various symmetric and non-symmetric sandwich beams with FG material in the core or skins under the uniformly distributed load are analysed. Numerical results are compared with those predicted by other theories to show the effects of shear deformation and thickness stretching on displacement and stresses.

2. FG sandwich beams

Consider a FG sandwich beam with length L and rectangular cross-section $b \times h$, with b being the width and h being the height. For simplicity, Poisson's ratio ν, is assumed to be constant, whereas, Young's modulus E is assumed to vary continuously with a power-law distribution [43]:

$$E(z) \quad = \quad (E_c - E_m)V_c + E_m \tag{1}$$

where subscripts m and c represent the metallic and ceramic constituents, V_c is volume fraction of the ceramic phase of the beam. Three types of FG beams are considered:

2.1. Type A: FG beams

The beam is composed of a FG material (Fig. 1a) with V_c given by:

$$V_c(z) = \left(\frac{2z+h}{2h}\right)^p, \quad z \in [-h/2, h/2] \tag{2}$$

where p is the power-law index.

2.2. Type B: sandwich beams with homogeneous skins - FG core

The bottom and top skin of sandwich beams is metal and ceramic, while, the core is composed of a FG material (Fig. 1b) with V_c given by [41]:

$$\begin{cases} V_c = 0, & z \in [-h/2, h_1] \quad \text{(bottom skin)} \\ V_c = \left(\frac{z-h_1}{h_2-h_1}\right)^p, & z \in [h_1, h_2] \quad \text{(core)} \\ V_c = 1, & z \in [h_2, h/2] \quad \text{(top skin)} \end{cases} \tag{3}$$

2.3. Type C: sandwich beams with FG skins - ceramic core

The bottom and top skin of sandwich beams is composed of a FG material, while, the core is ceramic (Fig. 1c) with V_c given by ([9],[10]):

$$\begin{cases} V_c = \left(\frac{z-h_o}{h_1-h_0}\right)^p, & z \in [-h/2, h_1] \quad \text{(bottom skin)} \\ V_c = 1, & z \in [h_1, h_2] \quad \text{(core)} \\ V_c = \left(\frac{z-h_3}{h_2-h_3}\right)^k, & z \in [h_2, h/2] \quad \text{(top skin)} \end{cases} \tag{4}$$

3. Kinematics

In order to include both shear deformation and thickness stretching effects, the axial and transverse displacements are assumed to be cubic and parabolic variation through the thickness [44]:

$$U(x,z) = u(x,t) - z\frac{dw_b(x)}{dx} - \frac{4z^3}{3h^2}\frac{dw_s(x)}{dx} = u(x) - zw_b'(x) - f(z)w_s'(x) \tag{5a}$$

$$W(x,z) = w_b(x) + w_s(x) + (1 - \frac{4z^2}{h^2})w_z(x) = w_b(x) + w_s(x) + g(z)w_z(x) \tag{5b}$$

where u, w_b, w_s and w_z are four unknown displacements of mid-plane of the beam. If component $g(z)w_z(x)$ is not included, Eq. (5) contains the displacement field of the Classical Beam Theory (CBT, $f = g = 0$), the First-order Beam Theory (FBT, $f = 0, g = 1$) and the Third-order Beam Theory (TBT, $f = \frac{4z^3}{3h^2}, g = 1 - \frac{4z^2}{h^2}$), here $g = 1 - f'$, which defines the distribution of the shear strains through the beam depth.

The only non-zero strains are:

$$\epsilon_x = \frac{\partial U}{\partial x} = u' - zw_b'' - fw_s'' \tag{6a}$$

$$\epsilon_z = \frac{\partial W}{\partial z} = g'w_z \tag{6b}$$

$$\gamma_{xz} = \frac{\partial W}{\partial x} + \frac{\partial U}{\partial z} = g(w_s' + w_z') \tag{6c}$$

4. Variational Formulation

The variation of the strain energy can be stated as:

$$\begin{aligned}\delta\mathcal{U} &= \int_0^l \int_0^b \left[\int_{-h/2}^{h/2} (\sigma_x \delta\epsilon_x + \sigma_{xz}\delta\gamma_{xz} + \sigma_z g' \delta w_z) dz \right] dy dx \\ &= \int_0^l \left[N_x \delta u' - M_x^b \delta w_b'' - M_x^s \delta w_s'' + Q_{xz}(\delta w_s' + \delta w_z') + R_z \delta w_z \right]) dx \end{aligned} \tag{7}$$

where $N_x, M_x^b, M_x^s, Q_{xz}$ and R_z are the stress resultants, defined as:

$$N_x = \int_{-h/2}^{h/2} \sigma_x b dz \tag{8a}$$

$$M_x^b = \int_{-h/2}^{h/2} \sigma_x z b dz \tag{8b}$$

$$M_x^s = \int_{-h/2}^{h/2} \sigma_x f b dz \tag{8c}$$

$$Q_{xz} = \int_{-h/2}^{h/2} \sigma_{xz} g b dz \tag{8d}$$

$$R_z = \int_{-h/2}^{h/2} \sigma_z g' b dz \tag{8e}$$

The variation of the potential energy under a transverse load q can be written as

$$\delta\mathcal{V} = -\int_0^l q(\delta w_b + \delta w_s) dx \tag{9}$$

By using the principle of total potential energy, the following weak statement is obtained:

$$0 = \int_0^l \left[N_x \delta u' - M_x^b \delta w_b'' - M_x^s \delta w_s'' + Q_{xz}(\delta w_s' + \delta w_z') + R_z \delta w_z - q(\delta w_b + \delta w_s) \right] dx \tag{10}$$

5. Constitutive Equations

The linear constitutive relations are given as:

$$\begin{Bmatrix} \sigma_x \\ \sigma_z \\ \sigma_{xz} \end{Bmatrix} = \begin{bmatrix} \bar{C}_{11}^* & \bar{C}_{13}^* & 0 \\ \bar{C}_{13}^* & \bar{C}_{11}^* & 0 \\ 0 & 0 & C_{55} \end{bmatrix} \begin{Bmatrix} \epsilon_x \\ \epsilon_z \\ \gamma_{xz} \end{Bmatrix} \tag{11}$$

where

$$\bar{C}_{11}^* = \bar{C}_{11} - \frac{\bar{C}_{12}^2}{\bar{C}_{22}} = \frac{E(z)}{1-\nu^2} \tag{12a}$$

$$\bar{C}_{13}^* = \bar{C}_{13} - \frac{\bar{C}_{12}\bar{C}_{23}}{\bar{C}_{22}} = \frac{E(z)\nu}{1-\nu^2} \tag{12b}$$

$$C_{55} = \frac{E(z)}{2(1+\nu)} \tag{12c}$$

If the thickness stretching effect is omitted ($\epsilon_z = 0$), elastic constants C_{ij} in Eq. (12) are reduced as:

$$\bar{C}^*_{11} = E(z) \tag{13a}$$

$$\bar{C}^*_{13} = 0 \tag{13b}$$

$$C_{55} = \frac{E(z)}{2(1+\nu)} \tag{13c}$$

By substituting Eqs. (11) and (6) into Eq. (8), the stress resultants can be expressed:

$$\begin{Bmatrix} N_x \\ M^b_x \\ M^s_x \\ R_z \\ Q_{xz} \end{Bmatrix} = \begin{bmatrix} A & B & B_s & X & 0 \\ & D & D_s & Y & 0 \\ & & H & Y_s & 0 \\ & & & Z & 0 \\ sym. & & & & A_s \end{bmatrix} \begin{Bmatrix} u' \\ -w''_b \\ -w''_s \\ w_z \\ w'_s + w'_z \end{Bmatrix} \tag{14}$$

where

$$(A, B, B_s, D, D_s, H, Z) = \int_{-h/2}^{h/2} \bar{C}^*_{11}(1, z, f, z^2, fz, f^2, g'^2) b dz \tag{15a}$$

$$A_s = \int_{-h/2}^{h/2} C_{55} g^2 b dz \tag{15b}$$

$$(X, Y, Y_s) = \int_{-h/2}^{h/2} \bar{C}^*_{13} g'(1, z, f) b dz \tag{15c}$$

6. Governing Equations

The governing equations can be obtained by integrating the derivatives of the varied quantities by parts and collecting the coefficients of $\delta u, \delta w_b, \delta w_s$ and δw_z:

$$N'_x = 0 \tag{16a}$$

$$M^{b\prime\prime}_x + q = 0 \tag{16b}$$

$$M^{s\prime\prime}_x + Q'_{xz} + q = 0 \tag{16c}$$

$$Q'_{xz} - R_z = 0 \tag{16d}$$

The natural boundary conditions are of the form:

$$\delta u \quad : \quad N_x \tag{17a}$$

$$\delta w_b \;:\; M_x^{b\prime} \tag{17b}$$

$$\delta w_b' \;:\; M_x^{b} \tag{17c}$$

$$\delta w_s \;:\; M_x^{s\prime} + Q_{xz} \tag{17d}$$

$$\delta w_s' \;:\; M_x^{s} \tag{17e}$$

$$\delta w_z \;:\; Q_{xz} \tag{17f}$$

By substituting Eq. (14) into Eq. (16), the governing equations can be expressed:

$$Au'' - Bw_b''' - B_s w_s''' + Xw_z' = 0 \tag{18a}$$

$$Bu''' - Dw_b^{iv} - D_s w_s^{iv} + Yw_z'' + q = 0 \tag{18b}$$

$$B_s u''' - D_s w_b^{iv} - Hw_s^{iv} + A_s w_s'' + (A_s + Y_s)w_z'' + q = 0 \tag{18c}$$

$$-Xu' + Yw_b'' + (A_s + Y_s)w_s'' + A_s w_z'' - Zw_z = 0 \tag{18d}$$

7. Solution Procedure

7.1. Analytical Solutions

For simply-supported boundary conditions, the Navier solution is assumed to be of the form:

$$u(x) = \sum_n^\infty U_n \cos\alpha x \tag{19a}$$

$$w_b(x) = \sum_n^\infty W_{bn} \sin\alpha x \tag{19b}$$

$$w_s(x) = \sum_n^\infty W_{sn} \sin\alpha x \tag{19c}$$

$$w_z(x) = \sum_n^\infty W_{zn} \sin\alpha x \tag{19d}$$

where $\alpha = n\pi/L$ and U_n, W_{bn}, W_{sn} and W_{zn} are the coefficients.

The transverse load q is also expanded in Fourier series for an uniform load (q_o) as:

$$q(x) = \sum_n^\infty Q_n \sin\alpha x = \sum_n^\infty \frac{4q_o}{n\pi} \sin\alpha x \quad \text{with} \quad n = 1, 3, 5, ... \tag{20}$$

By substituting Eqs. (19) and (20) into Eq. (18), the analytical solution can be obtained from the following equations:

$$\begin{bmatrix} S_{11} & S_{12} & S_{13} & S_{14} \\ & S_{22} & S_{23} & S_{24} \\ & & S_{33} & S_{34} \\ \text{sym.} & & & S_{44} \end{bmatrix} \begin{Bmatrix} U_n \\ W_{bn} \\ W_{sn} \\ W_{zn} \end{Bmatrix} = \begin{Bmatrix} 0 \\ Q_n \\ Q_n \\ 0 \end{Bmatrix} \tag{21}$$

where

$$S_{11} = A\alpha^2; \quad S_{12} = -B\alpha^3; \quad S_{13} = -B_s\alpha^3; \quad S_{14} = -X\alpha \tag{22a}$$

$$S_{22} = D\alpha^4; \quad S_{23} = D_s\alpha^4; \quad S_{24} = Y\alpha^2 \tag{22b}$$

$$S_{33} = A_s\alpha^2 + H\alpha^4; \quad S_{34} = (A_s + Y_s)\alpha^2; \quad S_{44} = A_s\alpha^2 + Z \tag{22c}$$

7.2. Finite Element Formulation

A two-noded C^1 beam element with six degree-of-freedom per node is developed. Linear polynomial Ψ_j is used for u and w_z and Hermite-cubic polynomial ψ_j is used for w_b and w_s. The generalized displacements within an element are expressed as:

$$u = \sum_{j=1}^{2} u_j \Psi_j \tag{23a}$$

$$w_b = \sum_{j=1}^{4} w_{bj} \psi_j \tag{23b}$$

$$w_s = \sum_{j=1}^{4} w_{sj} \psi_j \tag{23c}$$

$$w_z = \sum_{j=1}^{2} w_{zj} \Psi_j \tag{23d}$$

By substituting Eq. (23) into Eq. (10), the finite element model of a typical element can be expressed as:

$$\begin{bmatrix} K_{ij}^{11} & K_{ij}^{12} & K_{ij}^{13} & K_{ij}^{14} \\ & K_{ij}^{22} & K_{ij}^{23} & K_{ij}^{24} \\ & & K_{ij}^{33} & K_{ij}^{34} \\ \text{sym.} & & & K_{ij}^{44} \end{bmatrix} \begin{Bmatrix} U \\ W_b \\ W_s \\ W_z \end{Bmatrix} = \begin{Bmatrix} 0 \\ F_i^2 \\ F_i^3 \\ 0 \end{Bmatrix} \tag{24}$$

where

$$K_{ij}^{11} = \int_0^l A\Psi_i'\Psi_j' dx; \quad K_{ij}^{12} = -\int_0^l B\Psi_i'\psi_j'' dx \tag{25a}$$

$$K_{ij}^{13} = -\int_0^l B_s\Psi_i'\psi_j'' dx; \quad K_{ij}^{14} = \int_0^l X\Psi_i'\Psi_j dx \tag{25b}$$

$$K_{ij}^{22} = \int_0^l D\psi_i''\psi_j'' dx; \quad K_{ij}^{23} = \int_0^l D_s\psi_i''\psi_j'' dx; \quad K_{ij}^{24} = -\int_0^l Y\psi_i''\Psi_j dx \tag{25c}$$

$$K_{ij}^{33} = \int_0^l (A_s\psi_i'\psi_j' + H\psi_i''\psi_j'') dx; \quad K_{ij}^{34} = \int_0^l (A_s\psi_i'\Psi_j' - Y_s\psi_i''\Psi_j) dx \tag{25d}$$

$$K_{ij}^{44} = \int_0^l (A_s \Psi_i' \Psi_j' + Z \Psi_i \Psi_j) dx; \quad F_i^2 = \int_0^l q \psi_i dx; \quad F_i^3 = \int_0^l q \psi_i dx \tag{25e}$$

8. Numerical Examples

In this section, the Navier and FEM solutions are used to investigate bending hehaviour of FG sandwich beams with various theories (CBT, FBT, TBT and quasi-3D). Displacements and stresses of symmetric and non-symmetric sandwich beams with FG material in the core or skins are calculated. Various power-law indexes, skin-core-skin thickness ratios and boundary conditions are considered. Unless mentioned otherwise, FG sandwich beams made of Aluminum as metal (Al: $E_m = 70\text{GPa}, \nu_m = 0.3$) and Alumina as ceramic (Al_2O_3: $E_c = 380\text{GPa}, \nu_c = 0.3$) with two slenderness ratios, $L/h = 5$ and 20, are considered. For convenience, the following non-dimensional terms are used, the vertical displacement of beams under an uniformly distributed load q:

$$\overline{w} = \begin{cases} \dfrac{100 E_m h^3}{q L^4} W(\dfrac{L}{2}, z) & \text{for S-S and C-C beams} \\ \dfrac{100 E_m h^3}{q L^4} W(L, z) & \text{for C-F beams} \end{cases} \tag{26}$$

and the axial, normal and shear stresses:

$$\overline{\sigma}_x = \frac{h}{qL} \sigma_x(\frac{L}{2}, z) \tag{27a}$$

$$\overline{\sigma}_z = \frac{h}{qL} \sigma_z(\frac{L}{2}, z) \tag{27b}$$

$$\overline{\sigma}_{xz} = \frac{h}{qL} \sigma_{xz}(0, z) \tag{27c}$$

as well as parameters α_s and α_z, which are defined to assess the shear deformation and thickness stretching effects:

$$\alpha_s = \frac{w_s}{w} \tag{28a}$$

$$\alpha_z = \frac{w_z}{w} \tag{28b}$$

8.1. FG beams

As the first example, FG beams (Type A) under an uniformly distributed load are considered. The maximum displacements and stresses obtained from the different theories for various boundary conditions are given in Tables 1-5 along with the results from previous studies ([21], [22]) using CBT and TBT. It is clear that the results by Navier solutions agree completely with those of previous paper [22]. The comparisons of the vertical displacement and stresses through the thickness of present theory

and previous paper [22] using TBT are also plotted in Figs. 2-4. Tables 1-4 show that the results from FEM and Navier solutions are very close especially with the vertical displacement and normal stress. It can be observed that the current results are in excellent agreement with previous studies, thus accuracy of the present model is established. The normal stress in Table 2, which highlights the thickness stretching effect on bending behaviour of beam, is never obtained from CBT, FBT and TBT. Due to this effect, the vertical displacement and shear stress from the present quasi-3D theory ($\epsilon_z \neq 0$) are slightly smaller than those obtained from TBT ($\epsilon_z = 0$) (Figs. 2 and 3). Variations of the shear deformation and thickness stretching parameters with respect to the power-law index and slenderness ratio for various boundary conditions are plotted in Figs. 5 and 6. It can be seen that these parameters depend not only on the power-law index, slenderness ratio but also boundary conditions, which is more pronounced for clamped-clamped (C-C) and simply-supported (S-S) beams than clamped-free (C-F) one. For C-C beams with $L/h = 5$, as the power-law index increases, the shear deformation parameter decreases to the minimum value around $p = 0.8$ and increases to the maximum one around $p = 10.4$, and finally decreases (Fig. 5a). As the slenderness ratio increases, shear deformation and thickness stretching parameters decrease (Fig. 6).

8.2. Sandwich beams with homogeneous skins - FG core

In this example, bending analysis of (1-8-1) sandwich beams of Type B is performed. The results are given in Tables 6-9 and plotted in Figs. 7-9. It can be seen again that the results by Navier and FEM are in good agreement. Variation of shear shear deformation parameter for this type is a little different from previous example. From $p = 0$, this parameter decreases to minimum value around $p = 0.4$ and then increases with the increase of p (Fig. 6a). The thickness stretching parameter is maximum when $p = 0$ (Fig. 6b). The vertical displacements using the present quasi-3D theory, which includes normal strain, are again less than those of FBT and TBT. As the power-law index increases, they increase (Fig. 8 and Table 6). Fig. 9 shows the variation of the axial, shear and normal stresses through the thickness for different values of power-law index. The beam with $p = 10$ yields the maximum tensile axial stress at the top (ceramic-rich) surface and the maximum shear stress at the top surface of core layer (Fig. 9b). However, at the top surface of this beam ($p = 10$), the normal stress almost vanishes, whereas the maximum tensile normal stress occurs here with $p = 2$ (Fig. 9c).

8.3. Sandwich beams with FG skins - ceramic core

Finally, four types of symmetric (1-1-1, 1-2-1) and non-symmetric (2-1-1, 2-2-1) sandwich beams of Type C are considered. The vertical displacement for various boundary conditions are given in Tables 10-12 and plotted in Fig. 10. As expected, the CBT underestimates displacement. The difference

between the present quasi-3D theory and FBT, TBT is significant for thick beams ($L/h = 5$), but becomes negligible for thin ones ($L/h = 20$). The smallest and largest displacement correspond to the (1-2-1) and (2-1-1) sandwich beams since they have the highest and lowest portion of ceramic phase comparing with others. It is clear that in Tables 13-15, the ceramic beams ($p = 0$) give the smallest shear stress and the largest axial stress and normal stress. As the power-law index increases, $\overline{\sigma}_{xz}$ increases, whereas $\overline{\sigma}_x$ decreases and $\overline{\sigma}_z$ is variable. Their variations through the thickness are plotted in Figs. 11-13. There are some difference between the stresses of symmetric and non-symmetric beams. For symmetric beams (Figs. 11a,b and 12a,b), the same maximum tensile (compressive) axial and normal stress at the top (bottom) surface of core layer is observed. However, for non-symmetric ones, the maximum tensile axial stress occurs at the top surface of core layer and while the maximum compressive normal stress occurs at the bottom surface of core layer. It is interesting to see that the maximum shear stress for both symmetric and non-symmetric beams occurs at the mid-plane of the beam (Fig. 13).

9. Conclusions

Based on a quasi-3D theory, finite element model and Navier solutions are developed to determine the displacement and stresses of FG sandwich beams. This theory includes both shear deformation and thickness stretching effects. Various types of symmetric and non-symmetric sandwich beams are considered. Numerical results are compared with those predicted by other theories to show the effects of shear deformation and thickness stretching on the displacement and stresses. Effect of normal strain is important and should be considered in static behaviour of sandwich beams.

10. Acknowledgements

Authors gratefully acknowledge research support fund by UoA16 from Northumbria University and by the Basic Research Laboratory Program of the National Research Foundation of Korea(NRF) funded by the Ministry of Education, Science and Technology (2010-0019373 and 2012R1A2A1A01007450).

References

[1] F. Tornabene, J. N. Reddy, FGM and Laminated Doubly-Curved and degenerate Shells resting on Nonlinear Elastic Foundation: a GDQ Solution for Static Analysis with a Posteriori Stress and strain Recovery, Journal of Indian Institute of Science 93 (4) (2013) 635–688.

[2] E. Viola, L. Rossetti, N. Fantuzzi, F. Tornabene, Static analysis of functionally graded conical shells and panels using the generalized unconstrained third order theory coupled with the stress recovery, Composite Structures 112 (0) (2014) 44 – 65.

[3] F. A. Fazzolari, A refined dynamic stiffness element for free vibration analysis of cross-ply laminated composite cylindrical and spherical shallow shells, Composites Part B: Engineering 62 (0) (2014) 143 – 158.

[4] L. F. Qian, R. C. Batra, L. M. Chen, Static and dynamic deformations of thick functionally graded elastic plates by using higher-order shear and normal deformable plate theory and meshless local Petrov-Galerkin method, Composites Part B: Engineering 35 (6-8) (2004) 685 – 697.

[5] A. J. M. Ferreira, R. C. Batra, C. M. C. Roque, L. F. Qian, P. A. L. S. Martins, Static analysis of functionally graded plates using third-order shear deformation theory and a meshless method, Composite Structures 69 (4) (2005) 449 – 457.

[6] A. M. Zenkour, Generalized shear deformation theory for bending analysis of functionally graded plates, Applied Mathematical Modelling 30 (1) (2006) 67 – 84.

[7] H.-T. Thai, T. P. Vo, A new sinusoidal shear deformation theory for bending, buckling, and vibration of functionally graded plates, Applied Mathematical Modelling 37 (5) (2013) 3269 – 3281.

[8] M. Shariyat, K. Asemi, Three-dimensional non-linear elasticity-based 3D cubic B-spline finite element shear buckling analysis of rectangular orthotropic FGM plates surrounded by elastic foundations, Composites Part B: Engineering 56 (0) (2014) 934 – 947.

[9] A. M. Zenkour, A comprehensive analysis of functionally graded sandwich plates: Part 1-deflection and stresses, International Journal of Solids and Structures 42 (18-19) (2005) 5224 – 5242.

[10] A. M. Zenkour, A comprehensive analysis of functionally graded sandwich plates: Part 2-buckling and free vibration, International Journal of Solids and Structures 42 (18-19) (2005) 5243 – 5258.

[11] V.-H. Nguyen, T.-K. Nguyen, H.-T. Thai, T. P. Vo, A new inverse trigonometric shear deformation theory for isotropic and functionally graded sandwich plates, Composites Part B: Engineering 66 (0) (2014) 233–246.

[12] B. V. Sankar, An elasticity solution for functionally graded beams, Composites Science and Technology 61 (5) (2001) 689 – 696.

[13] A. Chakraborty, S. Gopalakrishnan, J. N. Reddy, A new beam finite element for the analysis of functionally graded materials, International Journal of Mechanical Sciences 45 (3) (2003) 519 – 539.

[14] X.-F. Li, A unified approach for analyzing static and dynamic behaviors of functionally graded Timoshenko and Euler-Bernoulli beams, Journal of Sound and Vibration 318 (4-5) (2008) 1210 – 1229.

[15] R. Kadoli, K. Akhtar, N. Ganesan, Static analysis of functionally graded beams using higher order shear deformation theory, Applied Mathematical Modelling 32 (12) (2008) 2509 – 2525.

[16] M. Benatta, I. Mechab, A. Tounsi, E. A. Bedia, Static analysis of functionally graded short beams including warping and shear deformation effects, Computational Materials Science 44 (2) (2008) 765 – 773.

[17] S. Kapuria, M. Bhattacharyya, A. N. Kumar, Bending and free vibration response of layered functionally graded beams: A theoretical model and its experimental validation, Composite Structures 82 (3) (2008) 390 – 402.

[18] S. Ben-Oumrane, T. Abedlouahed, M. Ismail, B. B. Mohamed, M. Mustapha, A. B. E. Abbas, A theoretical analysis of flexional bending of Al/Al2O3 S-FGM thick beams, Computational Materials Science 44 (4) (2009) 1344 – 1350.

[19] M. Simsek, Static analysis of a functionally graded beam under a uniformly distributed load by Ritz method, International Journal of Engineering and Applied Sciences 1 (3) (2009) 1–11.

[20] G. Giunta, S. Belouettar, E. Carrera, Analysis of FGM Beams by Means of Classical and Advanced Theories, Mechanics of Advanced Materials and Structures 17 (8) (2010) 622–635.

[21] X.-F. Li, B.-L. Wang, J.-C. Han, A higher-order theory for static and dynamic analyses of functionally graded beams, Archive of Applied Mechanics 80 (2010) 1197–1212.

[22] H.-T. Thai, T. P. Vo, Bending and free vibration of functionally graded beams using various higher-order shear deformation beam theories, International Journal of Mechanical Sciences 62 (1) (2012) 57 – 66.

[23] T.-K. Nguyen, T. P. Vo, H.-T. Thai, Static and free vibration of axially loaded functionally graded beams based on the first-order shear deformation theory, Composites Part B: Engineering 55 (0) (2013) 147–157.

[24] J. Murin, M. Aminbaghai, J. Hrabovsky, V. Kutis, S. Kugler, Modal analysis of the FGM beams with effect of the shear correction function, Composites Part B: Engineering 45 (1) (2013) 1575 – 1582.

[25] T. P. Vo, H.-T. Thai, T.-K. Nguyen, F. Inam, Static and vibration analysis of functionally graded beams using refined shear deformation theory, Meccanica (2013) 1–14.

[26] T. P. Vo, H.-T. Thai, T.-K. Nguyen, A. Maheri, J. Lee, Finite element model for vibration and buckling of functionally graded sandwich beams based on a refined shear deformation theory, Engineering Structures 64 (0) (2014) 12 – 22.

[27] E. Carrera, S. Brischetto, M. Cinefra, M. Soave, Effects of thickness stretching in functionally graded plates and shells, Composites Part B: Engineering 42 (2) (2011) 123 – 133.

[28] A. M. Zenkour, Benchmark trigonometric and 3-D elasticity solutions for an exponentially graded thick rectangular plate, Archive of Applied Mechanics 77 (4) (2007) 197–214.

[29] M. Talha, B. N. Singh, Static response and free vibration analysis of FGM plates using higher order shear deformation theory , Applied Mathematical Modelling 34 (12) (2010) 3991 – 4011.

[30] J. N. Reddy, A general nonlinear third-order theory of functionally graded plates, International Journal of Aerospace and Lightweight Structures 1 (1) (2011) 1–21.

[31] A. M. A. Neves, A. J. M. Ferreira, E. Carrera, C. M. C. Roque, M. Cinefra, R. M. N. Jorge, C. M. M. Soares, A quasi-3D sinusoidal shear deformation theory for the static and free vibration analysis of functionally graded plates, Composites Part B: Engineering 43 (2) (2012) 711 – 725.

[32] A. M. A. Neves, A. J. M. Ferreira, E. Carrera, M. Cinefra, C. M. C. Roque, R. M. N. Jorge, C. M. M. Soares, A quasi-3D hyperbolic shear deformation theory for the static and free vibration analysis of functionally graded plates , Composite Structures 94 (5) (2012) 1814 – 1825.

[33] J. L. Mantari, C. G. Soares, Generalized hybrid quasi-3D shear deformation theory for the static analysis of advanced composite plates , Composite Structures 94 (8) (2012) 2561 – 2575.

[34] J. L. Mantari, C. G. Soares, A novel higher-order shear deformation theory with stretching effect for functionally graded plates, Composites Part B: Engineering 45 (1) (2013) 268 – 281.

[35] J. L. Mantari, C. G. Soares, Four-unknown quasi-3D shear deformation theory for advanced composite plates, Composite Structures 109 (2014) 231 – 239.

[36] A. M. Zenkour, A simple four-unknown refined theory for bending analysis of functionally graded plates, Applied Mathematical Modelling 37 (20-21) (2013) 9041 – 9051.

[37] H.-T. Thai, T. P. Vo, T. Q. Bui, T.-K. Nguyen, A quasi-3D hyperbolic shear deformation theory for functionally graded plates, Acta Mechanica (2013) 1–14.

[38] H.-T. Thai, S.-E. Kim, A simple quasi-3D sinusoidal shear deformation theory for functionally graded plates , Composite Structures 99 (0) (2013) 172 – 180.

[39] Z. Belabed, M. S. A. Houari, A. Tounsi, S. R. Mahmoud, O. A. Beg, An efficient and simple higher order shear and normal deformation theory for functionally graded material (FGM) plates, Composites Part B: Engineering 60 (0) (2014) 274 – 283.

[40] H.-T. Thai, D.-H. Choi, Improved refined plate theory accounting for effect of thickness stretching in functionally graded plates, Composites Part B: Engineering 56 (0) (2014) 705 – 716.

[41] A. M. A. Neves, A. J. M. Ferreira, E. Carrera, M. Cinefra, C. M. C. Roque, R. M. N. Jorge, C. M. M. Soares, Static, free vibration and buckling analysis of isotropic and sandwich functionally graded plates using a quasi-3D higher-order shear deformation theory and a meshless technique, Composites Part B: Engineering 44 (1) (2013) 657 – 674.

[42] A. M. Zenkour, Bending analysis of functionally graded sandwich plates using a simple four-unknown shear and normal deformations theory, Journal of Sandwich Structures and Materials 15 (6) (2013) 629–656.

[43] J. N. Reddy, Mechanics of laminated composite plates and shells: theory and analysis, CRC, 2004.

[44] J. N. Reddy, A simple higher-order theory for laminated composite plates, Journal of Applied Mechanics 51 (4) (1984) 745–752.

Figure 1: Geometry and coordinate of a FG sandwich beam.

Figure 2: Comparison of the vertical displacement through the thickness of FG S-S beams under uniform load (Type A, L/h=5).

Figure 3: Comparison of the shear stress through the thickness of FG S-S beams under uniform load (Type A, L/h=5).

Figure 4: Comparison of the axial stress through the thickness of FG S-S beams under uniform load (Type A, L/h=5).

Figure 5: Variation of the shear deformation and thickness stretching parameters with respect to the power-law index of FG beams (Type A, L/h=5 and 20).

Figure 6: Variation of the shear deformation and thickness stretching parameters with respect to the slenderness ratio of FG beams (Type A, L/h=5 and 20).

Figure 7: Variation of the shear deformation and thickness stretching parameters with respect to the power-law index of (1-8-1) FG sandwich beams (Type B, L/h=5 and 20).

Figure 8: Variation of vertical displacement through the thickness of (1-8-1) FG sandwich S-S beams under uniform load (Type B, L/h=5).

Figure 9: Variation of the stresses through the thickness of (1-8-1) FG sandwich S-S beams under uniform load (Type B, L/h=5).

Figure 10: Variation of the vertical displacement through the thickness of FG sandwich S-S beams under uniform load (Type C, L/h=5).

Figure 11: Variation of the axial stress through the thickness of FG sandwich S-S beams under uniform load (Type C, L/h=5).

Figure 12: Variation of the normal stress through the thickness of FG sandwich S-S beams under uniform load (Type C, L/h=5).

Figure 13: Variation of the shear stress through the thickness of FG sandwich S-S beams under uniform load (Type C, L/h=5).

Table 1: Comparison of the maximum vertical displacement of FG S-S beams (Type A).

Table 2: Comparison of the normal stress $\overline{\sigma}_z(L/2, h/2)$ of FG S-S beams (Type A).

Table 3: Comparison of the axial stress $\overline{\sigma}_x(L/2, h/2)$ of FG S-S beams (Type A).

Table 4: Comparison of the shear stress $\overline{\sigma}_{xz}(0, 0)$ of FG S-S beams (Type A).

Table 5: The maximum vertical displacement of FG C-C and C-F beams (Type A).

Table 6: The maximum vertical displacement of (1-8-1) FG sandwich beams (Type B).

Table 7: Comparison of the normal stresses $\overline{\sigma}_z(L/2, h/2)$ of (1-8-1) FG sandwich S-S beams (Type B).

Table 8: Comparison of the axial stress $\overline{\sigma}_x(L/2, h/2)$ of (1-8-1) FG sandwich S-S beams (Type B).

Table 9: Comparison of the shear stress $\overline{\sigma}_{xz}(0, 0)$ of (1-8-1) FG sandwich S-S beams (Type B).

Table 10: The maximum vertical displacement of FG sandwich S-S beams (Type C).

Table 11: The maximum vertical displacement of FG sandwich C-C beams (Type C).

Table 12: The maximum vertical displacement of FG sandwich C-F beams (Type C).

Table 13: Axial stress $\overline{\sigma}_x(L/2, h/2)$ of FG sandwich S-S beams (Type C).

Table 14: Normal stress $\overline{\sigma}_z(L/2, h/2)$ of FG sandwich S-S beams (Type C).

Table 15: Shear stress $\overline{\sigma}_{xz}(0, 0)$ of FG sandwich S-S beams (Type C).

CAPTIONS OF TABLES

Table 1: Comparison of the maximum vertical displacement of FG S-S beams (Type A).

Table 2: Comparison of the normal stress $\bar{\sigma}_z\left(\mathrm{L}/2,\mathrm{h}/2\right)$ of FG S-S beams (Type A).

Table 3: Comparison of the axial stress $\bar{\sigma}_x\left(\mathrm{L}/2,\mathrm{h}/2\right)$ of FG S-S beams (Type A).

Table 4: Comparison of the shear stress $\bar{\sigma}_{xz}\left(0,0\right)$ of FG S-S beams (Type A).

Table 5: The maximum vertical displacement of FG C-C and C-F beams (Type A).

Table 6: The maximum vertical displacement of (1-8-1) FG sandwich beams (Type B).

Table 7: Comparison of the normal stresses $\bar{\sigma}_z\left(\mathrm{L}/2,\mathrm{h}/2\right)$ of (1-8-1) FG sandwich S-S beams (Type B).

Table 8: Comparison of the axial stress $\bar{\sigma}_x\left(\mathrm{L}/2,\mathrm{h}/2\right)$ of (1-8-1) FG sandwich S-S beams (Type B).

Table 9: Comparison of the shear stress $\bar{\sigma}_{xz}\left(0,0\right)$ of (1-8-1) FG sandwich S-S beams (Type B).

Table 10: The maximum vertical displacement of FG sandwich S-S beams (Type C).

Table 11: The maximum vertical displacement of FG sandwich C-C beams (Type C).

Table 12: The maximum vertical displacement of FG sandwich C-F beams (Type C).

Table 13: Axial stress $\bar{\sigma}_x\left(\mathrm{L}/2,\mathrm{h}/2\right)$ of FG sandwich S-S beams (Type C).

Table 14: Normal stress $\bar{\sigma}_z\left(\mathrm{L}/2,\mathrm{h}/2\right)$ of FG sandwich S-S beams (Type C).

Table 15: Shear stress $\bar{\sigma}_{xz}\left(0,0\right)$ of FG sandwich S-S beams (Type C).

Table 1: Comparison of the maximum vertical displacement of FG S-S beams (Type A).

Method	Theory	ε_z	$p=0$	$p=1$	$p=2$	$p=5$	$p=10$
L/h=5							
Li et al. [10]	TBT	$=0$	3.1657	6.2599	8.0602	9.7802	10.8979
Navier	CBT	$=0$	2.8783	5.7746	7.4003	8.7508	9.6072
	FBT	$=0$	3.1657	6.2599	8.0303	9.6483	10.7194
	TBT	$=0$	3.1654	6.2594	8.0677	9.8281	10.9381
	Present	$\neq 0$	3.1397	6.1338	7.8606	9.6037	10.7578
FEM	CBT	$=0$	2.8783	5.7741	7.3994	8.7499	9.6066
	FBT	$=0$	3.1657	6.2595	8.0294	9.6474	10.7188
	TBT	$=0$	3.1654	6.2590	8.0668	9.8271	10.9375
	Present	$\neq 0$	3.1397	6.1334	7.8598	9.6030	10.7572
L/h=20							
Li et al. [10]	TBT	$=0$	2.8962	5.8049	7.4415	8.8151	9.6879
Navier	CBT	$=0$	2.8783	5.7746	7.4003	8.7508	9.6072
	FBT	$=0$	2.8962	5.8049	7.4397	8.8069	9.6767
	TBT	$=0$	2.8962	5.8049	7.4421	8.8182	9.6905
	Present	$\neq 0$	2.8947	5.7201	7.2805	8.6479	9.5749
FEM	CBT	$=0$	2.8783	5.7741	7.3994	8.7499	9.6066
	FBT	$=0$	2.8963	5.8045	7.4388	8.8060	9.6761
	TBT	$=0$	2.8963	5.8045	7.4412	8.8173	9.6899
	Present	$\neq 0$	2.8947	5.7197	7.2797	8.6471	9.5743

Table 2: Comparison of the normal stress $\bar{\sigma}_z\left(\mathrm{L}/2,\mathrm{h}/2\right)$ of FG S-S beams (Type A).

Method	Theory	ε_z	$p=0$	$p=1$	$p=2$	$p=5$	$p=10$
L/h=5							
Navier	Present	$\neq 0$	0.1352	0.0670	0.0925	0.0180	-0.0181
FEM	Present	$\neq 0$	0.1352	0.0672	0.0927	0.0183	-0.0179
L/h=20							
Navier	Present	$\neq 0$	0.0337	-0.5880	-0.6269	-1.1698	-1.5572
FEM	Present	$\neq 0$	0.0338	-0.5874	-0.6261	-1.1690	-1.5560

Table 3: Comparison of the axial stress $\bar{\sigma}_x\left(\mathrm{L}/2,\mathrm{h}/2\right)$ of FG S-S beams (Type A).

Method	Theory	ε_z	$p=0$	$p=1$	$p=2$	$p=5$	$p=10$
L/h=5							
Li et al. [10]	TBT	$=0$	3.8020	5.8837	6.8812	8.1030	9.7063
Navier	FBT	$=0$	3.7500	5.7959	6.7676	7.9428	9.5228
	TBT	$=0$	3.8020	5.8836	6.8826	8.1106	9.7122
	Present	$\neq 0$	3.8005	5.8812	6.8818	8.1140	9.7164
FEM	FBT	$=0$	3.7520	5.7990	6.7710	7.9470	9.5290
	TBT	$=0$	3.8040	5.8870	6.8860	8.1150	9.7170
	Present	$\neq 0$	3.8020	5.8840	6.8860	8.1190	9.7220
L/h=20							
Li et al. [10]	TBT	$=0$	15.0130	23.2054	27.0989	31.8112	38.1372
Navier	FBT	$=0$	15.0000	23.1834	27.0704	31.7711	38.0913
	TBT	$=0$	15.0129	23.2053	27.0991	31.8130	38.1385
	Present	$\neq 0$	15.0125	23.2046	27.0988	31.8137	38.1395
FEM	FBT	$=0$	15.0100	23.2000	27.0800	31.7900	38.1100
	TBT	$=0$	15.0200	23.2200	27.1100	31.8300	38.1600
	Present	$\neq 0$	15.0200	23.2200	27.1100	31.8300	38.1600

Table 4: Comparison of the shear stress $\bar{\sigma}_{xz}\left(0,0\right)$ of FG S-S beams (Type A).

Method	Theory	ε_z	$p=0$	$p=1$	$p=2$	$p=5$	$p=10$
L/h=5							
Li et al. [10]	TBT	$=0$	0.7500	0.7500	0.6787	0.5790	0.6436
Navier	FBT	$=0$	0.5976	0.5976	0.5085	0.3914	0.4279
	TBT	$=0$	0.7332	0.7332	0.6706	0.5905	0.6467
	Present	$\neq 0$	0.7233	0.7233	0.6622	0.5840	0.6396
FEM	FBT	$=0$	0.5850	0.5850	0.4978	0.3832	0.4189
	TBT	$=0$	0.7335	0.7335	0.6700	0.5907	0.6477
	Present	$\neq 0$	0.7291	0.7291	0.6661	0.5873	0.6439
L/h=20							
Li et al. [10]	TBT	$=0$	0.7500	0.7500	0.6787	0.5790	0.6436
Navier	FBT	$=0$	0.5976	0.5976	0.5085	0.3914	0.4279
	TBT	$=0$	0.7451	0.7451	0.6824	0.6023	0.6596
	Present	$\neq 0$	0.7432	0.7432	0.6809	0.6010	0.6583
FEM	FBT	$=0$	0.5850	0.5850	0.4978	0.3832	0.4189
	TBT	$=0$	0.7470	0.7470	0.6777	0.6039	0.6682
	Present	$\neq 0$	0.7466	0.7466	0.6776	0.6036	0.6675

Table 5: The maximum vertical displacement of FG C-C and C-F beams (Type A).

Boundary conditions	Theory	ε_z	$p=0$	$p=1$	$p=2$	$p=5$	$p=10$
L/h=5							
C-C	CBT	$=0$	0.5757	1.1545	1.4792	1.7492	1.9208
	FBT	$=0$	0.8630	1.6398	2.1092	2.6468	3.0331
	TBT	$=0$	0.8501	1.6179	2.1151	2.7700	3.1812
	Present	$\neq 0$	0.8327	1.5722	2.0489	2.6929	3.1058
C-F	CBT	$=0$	27.632	55.434	71.039	84.004	92.227
	FBT	$=0$	28.7811	57.3756	73.5593	87.5939	96.6757
	TBT	$=0$	28.7555	57.3323	73.6482	88.2044	97.4151
	Present	$\neq 0$	28.5524	56.2002	71.7295	86.1201	95.7582
L/h=20							
C-C	CBT	$=0$	0.576	1.154	1.479	1.749	1.921
	FBT	$=0$	0.5936	1.1848	1.5186	1.8053	1.9903
	TBT	$=0$	0.5933	1.1843	1.5203	1.8155	2.0027
	Present	$\neq 0$	0.5894	1.1613	1.4811	1.7731	1.9694
C-F	CBT	$=0$	27.632	55.434	71.039	84.004	92.227
	FBT	$=0$	27.7034	55.5556	71.1968	84.2282	92.5048
	TBT	$=0$	27.7029	55.5546	71.2051	84.2712	92.5571
	Present	$\neq 0$	27.6217	54.6285	69.5266	82.4836	91.2606

Table 6: The maximum vertical displacement of (1-8-1) FG sandwich beams (Type B).

Boundary conditions	Theory	ε_z	$p=0$	$p=1$	$p=2$	$p=5$	$p=10$
L/h=5							
S-S (Navier)	CBT	$=0$	3.6744	6.2343	7.3695	8.0992	8.2882
	FBT	$=0$	3.9873	6.7196	7.9641	8.8664	9.1721
	TBT	$=0$	3.9788	6.7166	8.0083	9.0691	9.4817
	Present	$\neq 0$	3.9374	6.5505	7.7721	8.8089	9.2426
S-S (FEM)	CBT	$=0$	3.6744	6.2336	7.3684	8.0980	8.2871
	FBT	$=0$	3.9872	6.7189	7.9630	8.8652	9.1710
	TBT	$=0$	3.9788	6.7166	8.0083	9.0691	9.4817
	Present	$\neq 0$	3.9374	6.5499	7.7711	8.8078	9.2417
C-C	CBT	$=0$	0.7348	1.2462	1.4728	1.6186	1.6566
	FBT	$=0$	1.0477	1.7315	2.0674	2.3859	2.5405
	TBT	$=0$	1.0273	1.7079	2.0825	2.5386	2.7866
	Present	$\neq 0$	1.0046	1.6539	2.0122	2.4595	2.7089
C-F	CBT	$=0$	35.2739	59.8465	70.7429	77.7471	79.5623
	FBT	$=0$	36.5255	61.7878	73.1211	80.8160	83.0979
	TBT	$=0$	36.4685	61.7373	73.2441	81.5334	84.2168
	Present	$\neq 0$	36.1509	60.2081	71.0316	79.0886	81.9813
L/h=20							
S-S (Navier)	CBT	$=0$	3.6744	6.2343	7.3695	8.0992	8.2882
	FBT	$=0$	3.6939	6.2646	7.4067	8.1471	8.3434
	TBT	$=0$	3.6934	6.2638	7.4085	8.1587	8.3619
	Present	$\neq 0$	3.6841	6.1383	7.2143	7.9435	8.1710
S-S (FEM)	CBT	$=0$	3.6744	6.2336	7.3684	8.0980	8.2871
	FBT	$=0$	3.6939	6.2639	7.4056	8.1459	8.3424
	TBT	$=0$	3.6934	6.2638	7.4085	8.1587	8.3619
	Present	$\neq 0$	3.6840	6.1377	7.2133	7.9425	8.1700
C-C	CBT	$=0$	0.7348	1.2462	1.4728	1.6186	1.6566
	FBT	$=0$	0.7544	1.2765	1.5100	1.6666	1.7118
	TBT	$=0$	0.7536	1.2759	1.5122	1.6784	1.7300
	Present	$\neq 0$	0.7472	1.2447	1.4669	1.6283	1.6843
C-F	CBT	$=0$	35.2739	59.8465	70.7429	77.7471	79.5623
	FBT	$=0$	35.3522	59.9678	70.8915	77.9389	79.7833
	TBT	$=0$	35.3495	59.9664	70.9018	77.9882	79.8588
	Present	$\neq 0$	35.1767	58.6432	68.9096	75.7851	77.8811

Table 7: Comparison of the normal stresses $\bar{\sigma}_z\left(\mathrm{L}/2,\mathrm{h}/2\right)$ of (1-8-1) FG sandwich S-S beams (Type B).

Method	Theory	ε_z	$p=0$	$p=1$	$p=2$	$p=5$	$p=10$
L/h=5							
Navier	Present	$\neq 0$	0.0872	0.1043	0.1277	0.0619	-0.0001
FEM	Present	$\neq 0$	0.0873	0.1045	0.1279	0.0622	-0.0001
L/h=20							
Navier	Present	$\neq 0$	-0.2904	-0.4373	-0.4179	-0.8042	-1.1450
FEM	Present	$\neq 0$	-0.2901	-0.4367	-0.4170	-0.8032	-1.1440

Table 8: Comparison of the axial stress $\bar{\sigma}_x\left(\mathrm{L}/2,\mathrm{h}/2\right)$ of (1-8-1) FG sandwich S-S beams (Type B).

Method	Theory	ε_z	$p=0$	$p=1$	$p=2$	$p=5$	$p=10$
L/h=5							
Navier	FBT	$=0$	4.4045	5.9215	6.4143	6.7326	7.0461
	TBT	$=0$	4.4636	6.0094	6.5256	6.8886	7.2229
	Present	$\neq 0$	4.4603	6.0069	6.5253	6.8927	7.2292
FEM	FBT	$=0$	4.4070	5.9250	6.4170	6.7360	7.0500
	TBT	$=0$	4.4660	6.0130	6.5290	6.8930	7.2270
	Present	$\neq 0$	4.4620	6.0100	6.5290	6.8970	7.2330
L/h=20							
Navier	FBT	$=0$	17.6180	23.6861	25.6572	26.9305	28.1842
	TBT	$=0$	17.6327	23.7080	25.6849	26.9694	28.2283
	Present	$\neq 0$	17.6318	23.7073	25.6848	26.9703	28.2298
FEM	FBT	$=0$	17.6300	23.7000	25.6700	26.9500	28.2000
	TBT	$=0$	17.6400	23.7200	25.7000	26.9800	28.2400
	Present	$\neq 0$	17.6400	23.7200	25.7000	26.9900	28.2500

Table 9: Comparison of the shear stress $\bar{\sigma}_{xz}\left(0,0\right)$ of (1-8-1) FG sandwich S-S beams (Type B).

Method	Theory	ε_z	$p=0$	$p=1$	$p=2$	$p=5$	$p=10$
L/h=5							
Navier	FBT	$=0$	0.6506	0.5976	0.4799	0.3346	0.3400
	TBT	$=0$	0.7597	0.7318	0.6445	0.5319	0.5792
	Present	$\neq 0$	0.7486	0.7219	0.6365	0.5262	0.5733
FEM	FBT	$=0$	0.6370	0.5850	0.4698	0.3275	0.3329
	TBT	$=0$	0.7611	0.7315	0.6432	0.5316	0.5798
	Present	$\neq 0$	0.7568	0.7272	0.6395	0.5286	0.5766
L/h=20							
Navier	FBT	$=0$	0.6506	0.5976	0.4799	0.3346	0.3400
	TBT	$=0$	0.7702	0.7436	0.6558	0.5425	0.5910
	Present	$\neq 0$	0.7683	0.7418	0.6543	0.5414	0.5900
FEM	FBT	$=0$	0.6370	0.5850	0.4698	0.3275	0.3329
	TBT	$=0$	0.7785	0.7416	0.6452	0.5400	0.5969
	Present	$\neq 0$	0.7777	0.7412	0.6454	0.5399	0.5963

Table 10: The maximum vertical displacement of FG sandwich S-S beams (Type C).

p	Theory	ε_z	L/h=5				L/h=20			
			1-1-1	1-2-1	2-1-1	2-2-1	1-1-1	1-2-1	2-1-1	2-2-1
0	CBT	$=0$	2.8783	2.8783	2.8783	2.8783	2.8783	2.8783	2.8783	2.8783
	FBT	$=0$	3.1657	3.1657	3.1657	3.1657	2.8963	2.8963	2.8963	2.8963
	TBT	$=0$	3.1654	3.1654	3.1654	3.1654	2.8963	2.8963	2.8963	2.8963
	Present	$\neq 0$	3.1397	3.1397	3.1397	3.1397	2.8947	2.8947	2.8947	2.8947
1	CBT	$=0$	5.9181	5.0798	6.1746	5.4944	5.9181	5.0798	6.1746	5.4944
	FBT	$=0$	6.3128	5.4408	6.5886	5.8749	5.9428	5.1024	6.2004	5.5182
	TBT	$=0$	6.2693	5.4122	6.5450	5.8403	5.9401	5.1006	6.1977	5.5161
	Present	$\neq 0$	6.2098	5.3612	6.4719	5.7777	5.9364	5.0975	6.1810	5.5040
2	CBT	$=0$	8.0074	6.4056	8.4744	7.1846	8.0074	6.4056	8.4744	7.1846
	FBT	$=0$	8.4582	6.8003	8.9597	7.6112	8.0356	6.4302	8.5047	7.2113
	TBT	$=0$	8.3893	6.7579	8.8896	7.5583	8.0313	6.4276	8.5003	7.2080
	Present	$\neq 0$	8.3069	6.6913	8.7701	7.4629	8.0262	6.4235	8.4572	7.1790
5	CBT	$=0$	10.8117	8.1409	11.3485	9.3867	10.8117	8.1409	11.3485	9.3867
	FBT	$=0$	11.3372	8.5762	11.9348	9.8720	10.8445	8.1681	11.3851	9.4170
	TBT	$=0$	11.2274	8.5137	11.8246	9.7919	10.8376	8.1642	11.3782	9.4120
	Present	$\neq 0$	11.1175	8.4276	11.6384	9.6459	10.8309	8.1589	11.2886	9.3498
10	CBT	$=0$	12.1322	9.0232	12.4957	10.4262	12.1322	9.0232	12.4957	10.4262
	FBT	$=0$	12.7006	9.4800	13.1433	10.9440	12.1677	9.0518	12.5362	10.4586
	TBT	$=0$	12.5659	9.4050	13.0135	10.8486	12.1593	9.0471	12.5281	10.4526
	Present	$\neq 0$	12.4453	9.3099	12.8026	10.6769	12.1519	9.0413	12.4206	10.3715

Table 11: The maximum vertical displacement of FG sandwich C-C beams (Type C).

p	Theory	ε_z	L/h=5				L/h=20			
			1-1-1	1-2-1	2-1-1	2-2-1	1-1-1	1-2-1	2-1-1	2-2-1
0	CBT	$=0$	0.5757	0.5757	0.5757	0.5757	0.5757	0.5757	0.5757	0.5757
	FBT	$=0$	0.8630	0.8630	0.8630	0.8630	0.5936	0.5936	0.5936	0.5936
	TBT	$=0$	0.8501	0.8501	0.8501	0.8501	0.5933	0.5933	0.5933	0.5933
	Present	$\neq 0$	0.8327	0.8327	0.8327	0.8327	0.5894	0.5894	0.5894	0.5894
1	CBT	$=0$	1.1836	1.0160	1.2349	1.0989	1.1836	1.0160	1.2349	1.0989
	FBT	$=0$	1.5783	1.3770	1.6489	1.4793	1.2083	1.0385	1.2607	1.1226
	TBT	$=0$	1.5232	1.3372	1.5930	1.4332	1.2053	1.0365	1.2577	1.1202
	Present	$\neq 0$	1.4889	1.3077	1.5554	1.4002	1.1968	1.0293	1.2465	1.1108
2	CBT	$=0$	1.6015	1.2811	1.6947	1.4368	1.6015	1.2811	1.6947	1.4368
	FBT	$=0$	2.0523	1.6758	2.1800	1.8634	1.6297	1.3058	1.7250	1.4635
	TBT	$=0$	1.9715	1.6225	2.0969	1.7988	1.6250	1.3028	1.7203	1.4599
	Present	$\neq 0$	1.9247	1.5853	2.0427	1.7540	1.6132	1.2936	1.7010	1.4450
5	CBT	$=0$	2.1623	1.6282	2.2693	1.8771	2.1623	1.6282	2.2693	1.8771
	FBT	$=0$	2.6879	2.0635	2.8556	2.3624	2.1952	1.6554	2.3060	1.9074
	TBT	$=0$	2.5652	1.9896	2.7306	2.2700	2.1880	1.6512	2.2987	1.9021
	Present	$\neq 0$	2.5013	1.9416	2.6539	2.2080	2.1715	1.6390	2.2668	1.8779
10	CBT	$=0$	2.4264	1.8046	2.4987	2.0849	2.4264	1.8046	2.4987	2.0849
	FBT	$=0$	2.9948	2.2614	3.1463	2.6027	2.4620	1.8332	2.5392	2.1173
	TBT	$=0$	2.8468	2.1747	3.0002	2.4945	2.4532	1.8282	2.5307	2.1110
	Present	$\neq 0$	2.7754	2.1211	2.9149	2.4242	2.4346	1.8145	2.4939	2.0818

Table 12: The maximum vertical displacement of FG sandwich C-F beams (Type C).

p	Theory	ε_z	L/h=5				L/h=20			
			1-1-1	1-2-1	2-1-1	2-2-1	1-1-1	1-2-1	2-1-1	2-2-1
0	CBT	$=0$	27.6316	27.6316	27.6316	27.6316	27.6316	27.6316	27.6316	27.6316
	FBT	$=0$	28.7811	28.7811	28.7811	28.7811	27.7034	27.7034	27.7034	27.7034
	TBT	$=0$	28.7555	28.7555	28.7555	28.7555	27.7029	27.7029	27.7029	27.7029
	Present	$\neq 0$	28.5524	28.5524	28.5524	28.5524	27.6217	27.6217	27.6217	27.6217
1	CBT	$=0$	56.8136	48.7663	59.2761	52.7467	56.8136	48.7663	59.2761	52.7467
	FBT	$=0$	58.3924	50.2103	60.9322	54.2687	56.9123	48.8566	59.3796	52.8419
	TBT	$=0$	58.1959	50.0741	60.7338	54.1078	56.9009	48.8489	59.3681	52.8327
	Present	$\neq 0$	57.7839	49.7281	60.1913	53.6540	56.7227	48.6985	59.0623	52.5878
2	CBT	$=0$	76.8709	61.4934	81.3552	68.9733	76.8709	61.4934	81.3552	68.9733
	FBT	$=0$	78.6742	63.0722	83.2965	70.6795	76.9836	61.5921	81.4765	69.0799
	TBT	$=0$	78.3753	62.8813	82.9905	70.4450	76.9658	61.5809	81.4583	69.0661
	Present	$\neq 0$	77.7957	62.4386	82.0520	69.7271	76.7147	61.3855	80.8432	68.6176
5	CBT	$=0$	103.7920	78.1525	108.9480	90.1141	103.7920	78.1525	108.9480	90.1141
	FBT	$=0$	105.8940	79.8939	111.2930	92.0554	103.9230	78.2614	109.0940	90.2354
	TBT	$=0$	105.4300	79.6213	110.8230	91.7109	103.8950	78.2451	109.0660	90.2148
	Present	$\neq 0$	104.5920	79.0288	109.2570	90.5335	103.5400	77.9869	107.9370	89.3942
10	CBT	$=0$	116.4690	86.6229	119.9620	100.0940	116.4690	86.6229	119.9620	100.0940
	FBT	$=0$	118.7420	88.4498	122.5520	102.1650	116.6110	86.7371	120.1240	100.2230
	TBT	$=0$	118.1780	88.1270	122.0020	101.7590	116.5770	86.7178	120.0910	100.1990
	Present	$\neq 0$	117.2190	87.4501	120.1930	100.3340	116.1730	86.4264	118.7640	99.1718

Table 13: Axial stress $\bar{\sigma}_x\left(\mathrm{L}/2,\mathrm{h}/2\right)$ of FG sandwich S-S beams (Type C).

p	Theory	ε_z	L/h=5				L/h=20			
			1-1-1	1-2-1	2-1-1	2-2-1	1-1-1	1-2-1	2-1-1	2-2-1
0	FBT	$=0$	3.7500	3.7500	3.7500	3.7500	15.0000	15.0000	15.0000	15.0000
	TBT	$=0$	3.8020	3.8020	3.8020	3.8020	15.0129	15.0129	15.0129	15.0129
	Present	$\neq 0$	3.8005	3.8005	3.8005	3.8005	15.0125	15.0125	15.0125	15.0125
1	FBT	$=0$	1.4203	1.2192	1.3730	1.2332	5.6814	4.8766	5.4922	4.9328
	TBT	$=0$	1.4349	1.2329	1.3884	1.2474	5.6850	4.8801	5.4960	4.9364
	Present	$\neq 0$	1.4330	1.2315	1.3866	1.2459	5.6845	4.8797	5.4955	4.9360
2	FBT	$=0$	1.9218	1.5373	1.8296	1.5712	7.6871	6.1493	7.3183	6.2849
	TBT	$=0$	1.9382	1.5527	1.8475	1.5873	7.6912	6.1532	7.3227	6.2889
	Present	$\neq 0$	1.9352	1.5505	1.8446	1.5849	7.6904	6.1526	7.3220	6.2882
5	FBT	$=0$	2.5948	1.9538	2.3864	2.0016	10.3792	7.8152	9.5457	8.0064
	TBT	$=0$	2.6123	1.9705	2.4069	2.0194	10.3835	7.8194	9.5508	8.0109
	Present	$\neq 0$	2.6079	1.9672	2.4030	2.0160	10.3824	7.8185	9.5498	8.0100
10	FBT	$=0$	2.9117	2.1656	2.6075	2.2015	11.6469	8.6623	10.4302	8.8058
	TBT	$=0$	2.9293	2.1826	2.6296	2.2199	11.6513	8.6665	10.4357	8.8104
	Present	$\neq 0$	2.9245	2.1788	2.6254	2.2161	11.6500	8.6655	10.4346	8.8094

Table 14: Normal stress $\bar{\sigma}_z\left(\mathrm{L}/2,\mathrm{h}/2\right)$ of FG sandwich S-S beams (Type C).

p	Theory	ε_z	L/h=5				L/h=20			
			1-1-1	1-2-1	2-1-1	2-2-1	1-1-1	1-2-1	2-1-1	2-2-1
0	Present	$\neq 0$	0.1352	0.1352	0.1352	0.1352	0.0337	0.0337	0.0337	0.0337
1	Present	$\neq 0$	0.0516	0.0447	0.0303	0.0286	0.0129	0.0111	-0.0757	-0.0625
2	Present	$\neq 0$	0.0693	0.0564	0.0389	0.0341	0.0173	0.0141	-0.1055	-0.0895
5	Present	$\neq 0$	0.0916	0.0712	0.0539	0.0454	0.0229	0.0178	-0.1158	-0.1010
10	Present	$\neq 0$	0.1013	0.0783	0.0589	0.0518	0.0253	0.0195	-0.1232	-0.0998

Table 15: Shear stress $\bar{\sigma}_{xz}\left(0,0\right)$ of FG sandwich S-S beams (Type C).

p	Theory	ε_z	L/h=5				L/h=20			
			1-1-1	1-2-1	2-1-1	2-2-1	1-1-1	1-2-1	2-1-1	2-2-1
0	FBT	$=0$	0.5976	0.5976	0.5976	0.5976	0.5976	0.5976	0.5976	0.5976
	TBT	$=0$	0.7332	0.7332	0.7332	0.7332	0.7451	0.7451	0.7451	0.7451
	Present	$\neq 0$	0.7233	0.7233	0.7233	0.7233	0.7432	0.7432	0.7432	0.7432
1	FBT	$=0$	0.8208	0.7507	0.8610	0.7912	0.8208	0.7507	0.8610	0.7912
	TBT	$=0$	0.8586	0.8123	0.9088	0.8479	0.8681	0.8215	0.9191	0.8575
	Present	$\neq 0$	0.8444	0.7993	0.8940	0.8342	0.8657	0.8193	0.9166	0.8552
2	FBT	$=0$	0.9375	0.8208	1.0092	0.8870	0.9375	0.8208	1.0092	0.8870
	TBT	$=0$	0.9249	0.8493	1.0136	0.9075	0.9344	0.8581	1.0242	0.9168
	Present	$\neq 0$	0.9084	0.8349	0.9961	0.8920	0.9316	0.8556	1.0212	0.9142
5	FBT	$=0$	1.0929	0.9053	1.2192	1.0092	1.0929	0.9053	1.2192	1.0092
	TBT	$=0$	1.0125	0.8925	1.1742	0.9859	1.0227	0.9014	1.1862	0.9957
	Present	$\neq 0$	0.9931	0.8763	1.1532	0.9683	1.0194	0.8986	1.1826	0.9927
10	FBT	$=0$	1.1819	0.9497	1.3465	1.0767	1.1819	0.9497	1.3465	1.0767
	TBT	$=0$	1.0665	0.9151	1.2875	1.0335	1.0773	0.9243	1.3008	1.0436
	Present	$\neq 0$	1.0458	0.8980	1.2646	1.0148	1.0736	0.9214	1.2969	1.0405

CAPTIONS OF FIGURES

Figure 1: Geometry and coordinate of a FG sandwich beam
Figure 2: Comparison of the vertical displacement through the thickness of FG S-S beams under uniform load (Type A, L/h=5).
Figure 3: Comparison of the shear stress through the thickness of FG S-S beams under uniform load (Type A, L/h=5).
Figure 4: Comparison of the axial stress through the thickness of FG S-S beams under uniform load (Type A, L/h=5).
Figure 5: Variation of the shear deformation and thickness stretching parameters with respect to the power-law index of FG beams (Type A, L/h=5 and 20).
Figure 6: Variation of the shear deformation and thickness stretching parameters with respect to the slenderness ratio of FG beams (Type A, L/h=5 and 20).
Figure 7: Variation of the shear deformation and thickness stretching parameters with respect to the power-law index of (1-8-1) FG sandwich beams (Type B, L/h=5 and 20).
Figure 8: Variation of the vertical displacement through the thickness of (1-8-1) FG sandwich S-S beams under uniform load (Type B, L/h=5).
Figure 9: Variation of the stresses through the thickness of (1-8-1) FG sandwich S-S beams under uniform load (Type B, L/h=5).
Figure 10: Variation of the vertical displacement through the thickness of FG sandwich S-S beams under uniform load (Type C, L/h=5).
Figure 11: Variation of the axial stress through the thickness of FG sandwich S-S beams under uniform load (Type C, L/h=5).
Figure 12: Variation of the normal stress through the thickness of FG sandwich S-S beams under uniform load (Type C, L/h=5).
Figure 13: Variation of the shear stress through the thickness of FG sandwich S-S beams under uniform load (Type C, L/h=5).

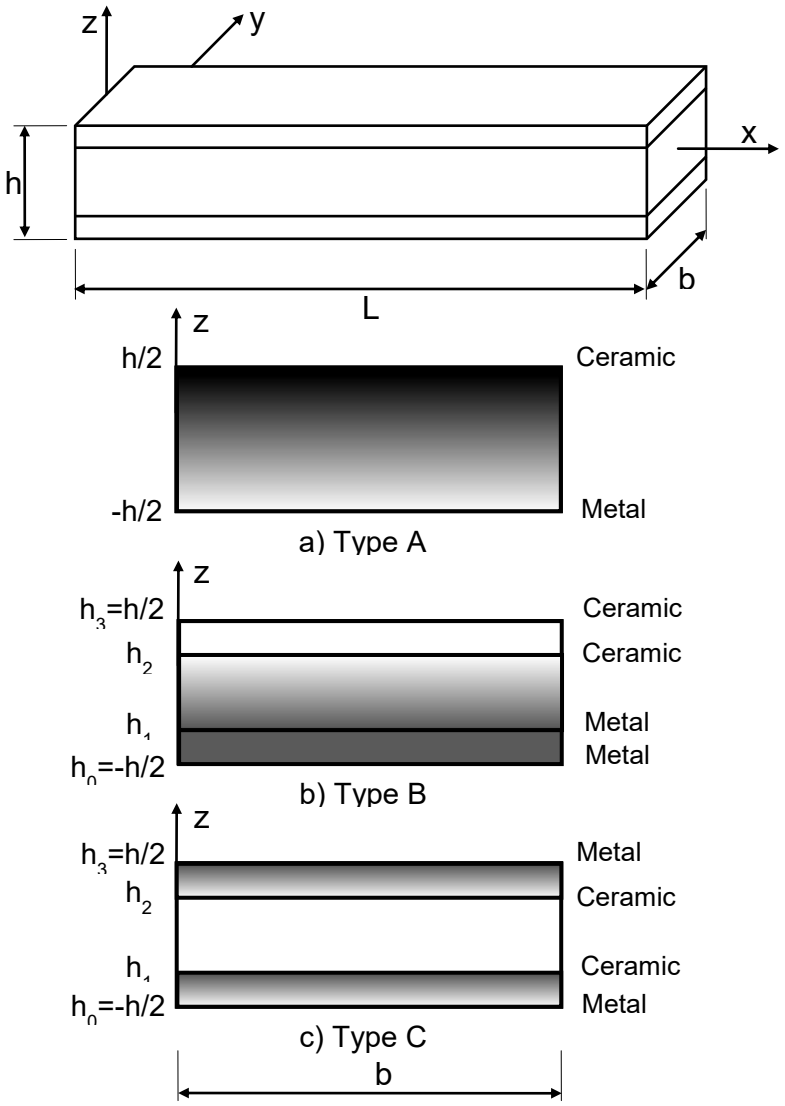

Figure 1: Geometry and coordinate of a FG sandwich beam

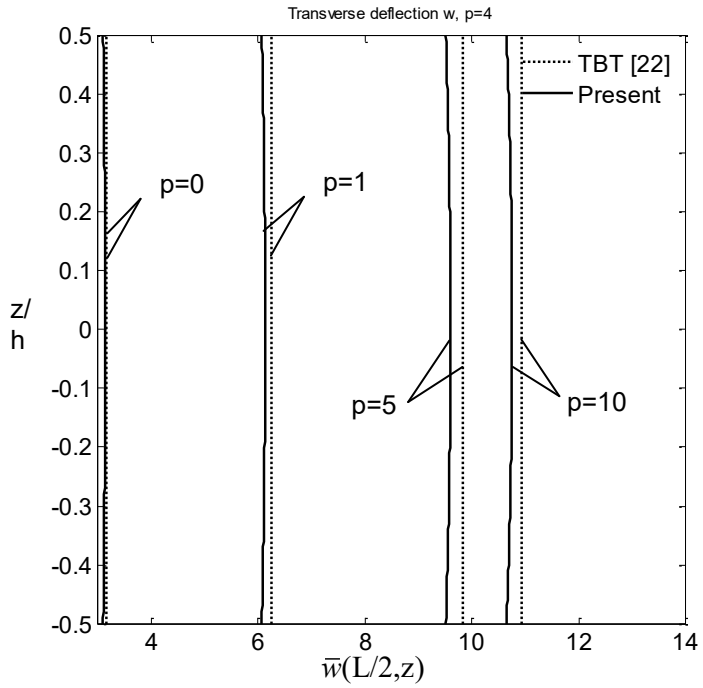

Figure 2: Comparison of the vertical displacement through the thickness of FG S-S beams under uniform load (Type A, L/h=5).

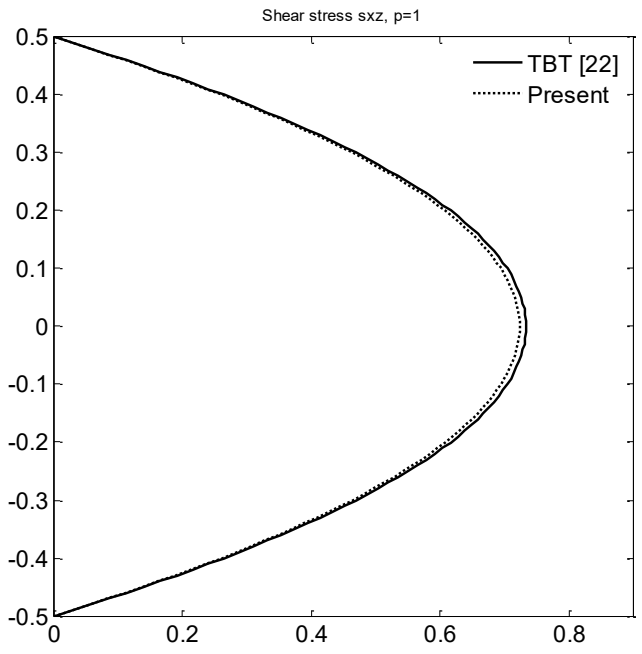

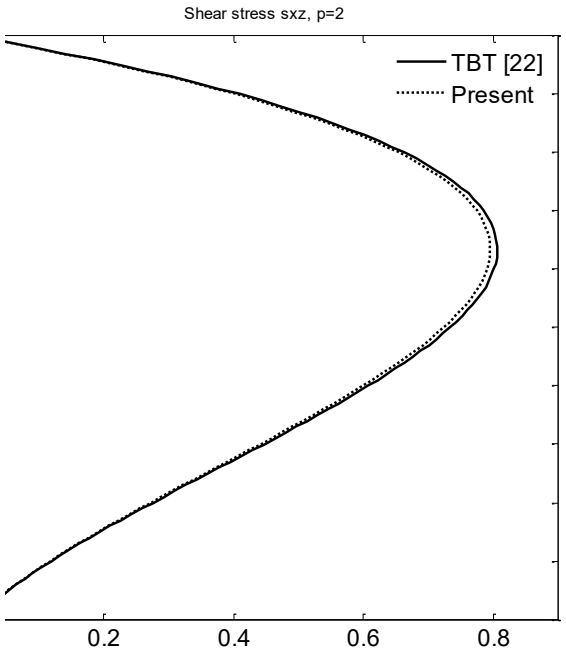

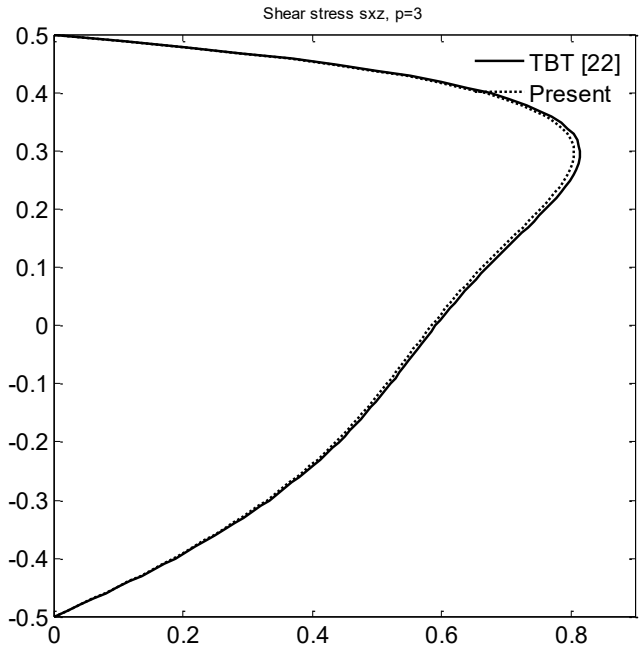

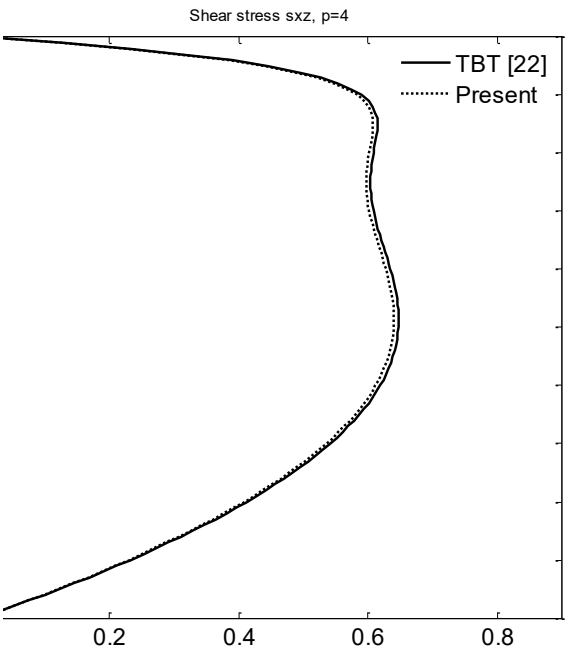

c) p=5 d) p=10

Figure 3: Comparison of the shear stress through the thickness of FG S-S beams under uniform load (Type A, L/h=5).

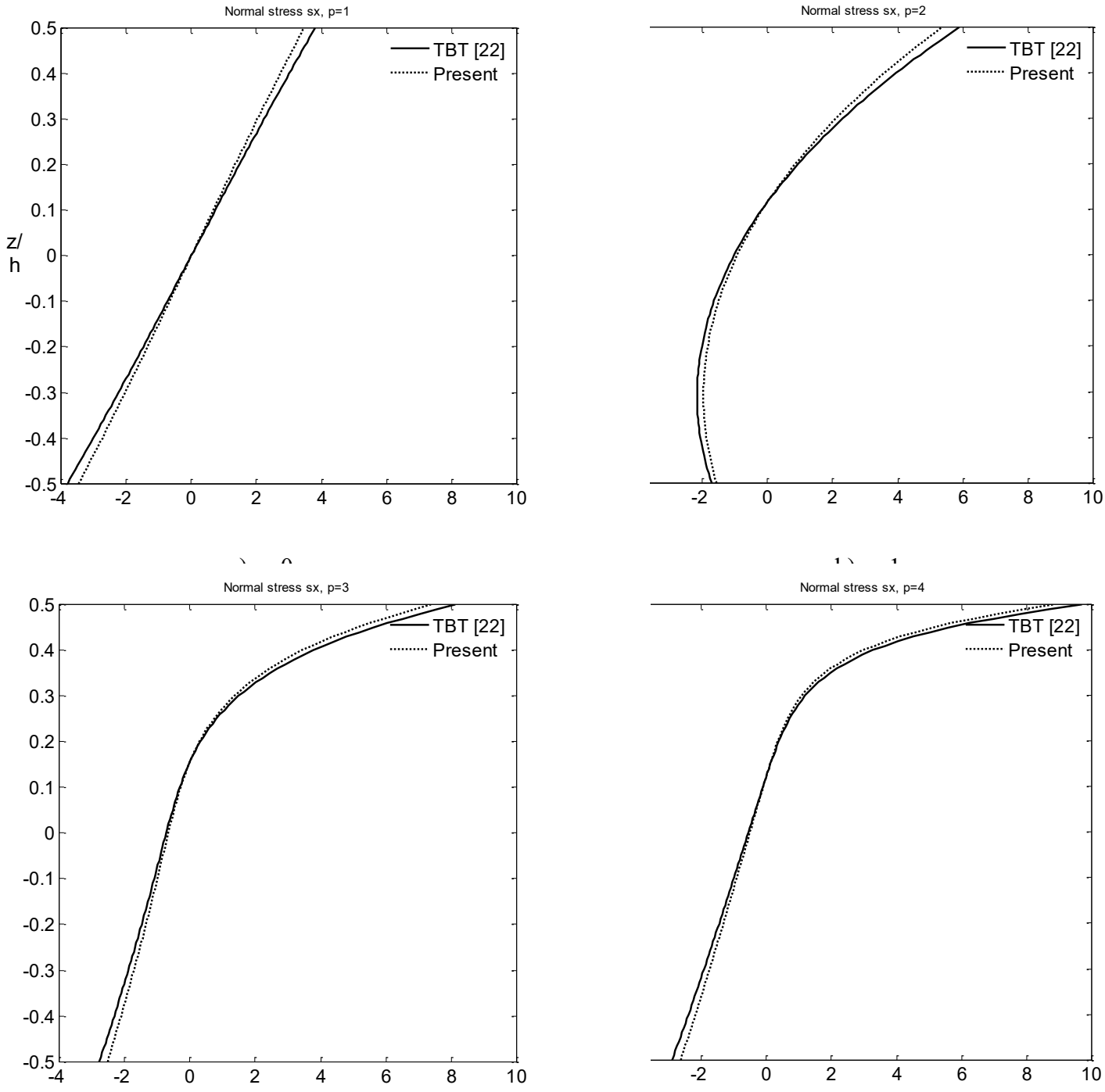

c) p=5 d) p=10

Figure 4: Comparison of the axial stress through the thickness of FG S-S beams under uniform load (Type A, L/h=5).

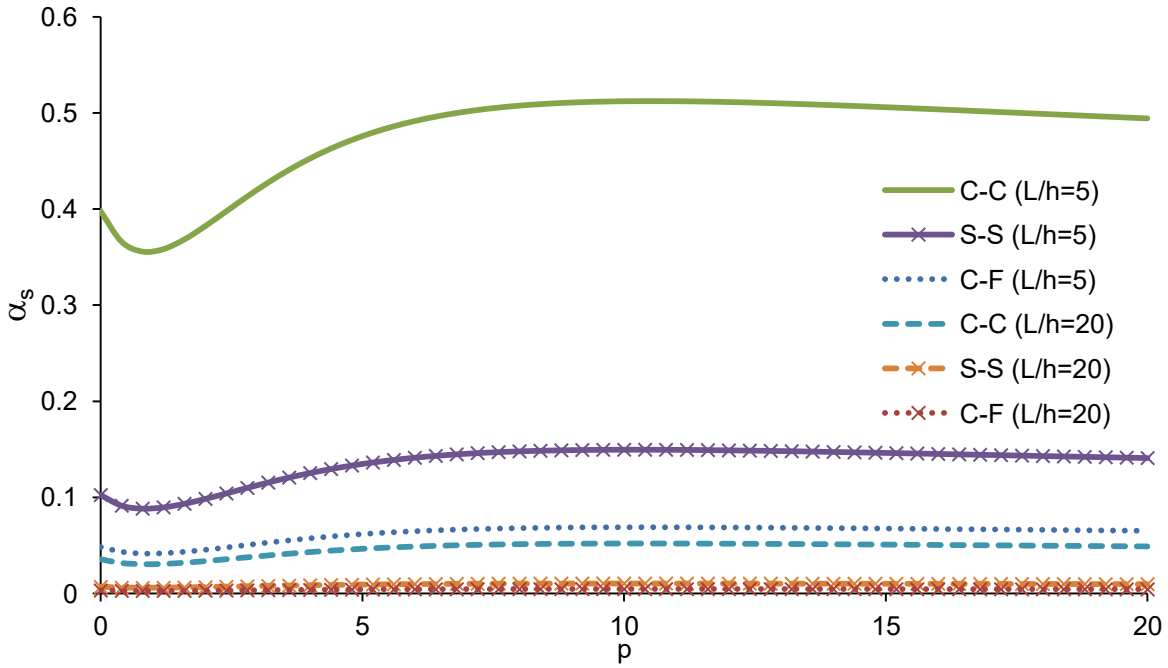

a. Shear deformation parameter.

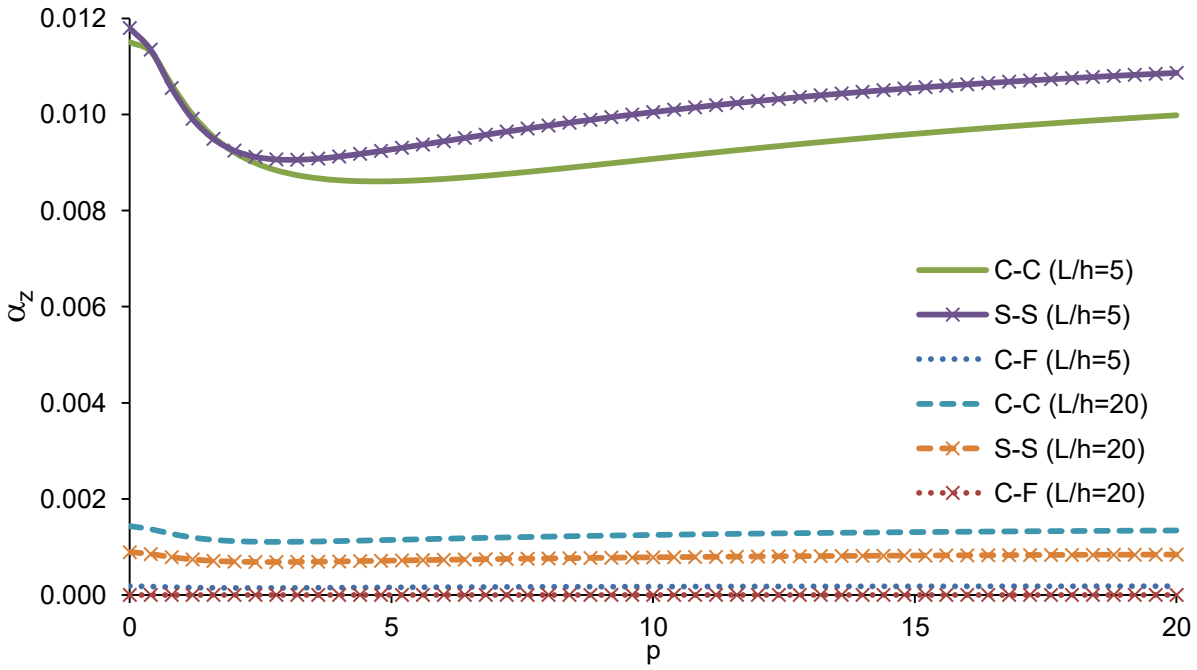

b. Thickness stretching parameter.

Figure 5: Variation of the shear deformation and thickness stretching parameters with respect to the power-law index of FG beams (Type A, L/h=5 and 20).

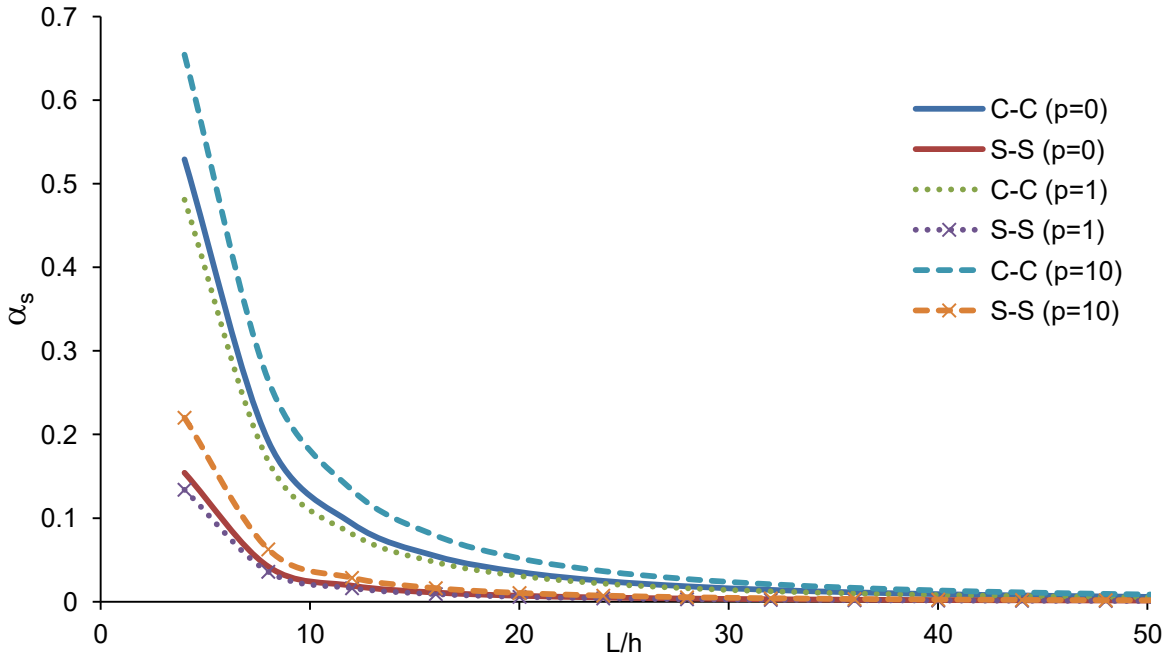

a. Shear deformation parameter.

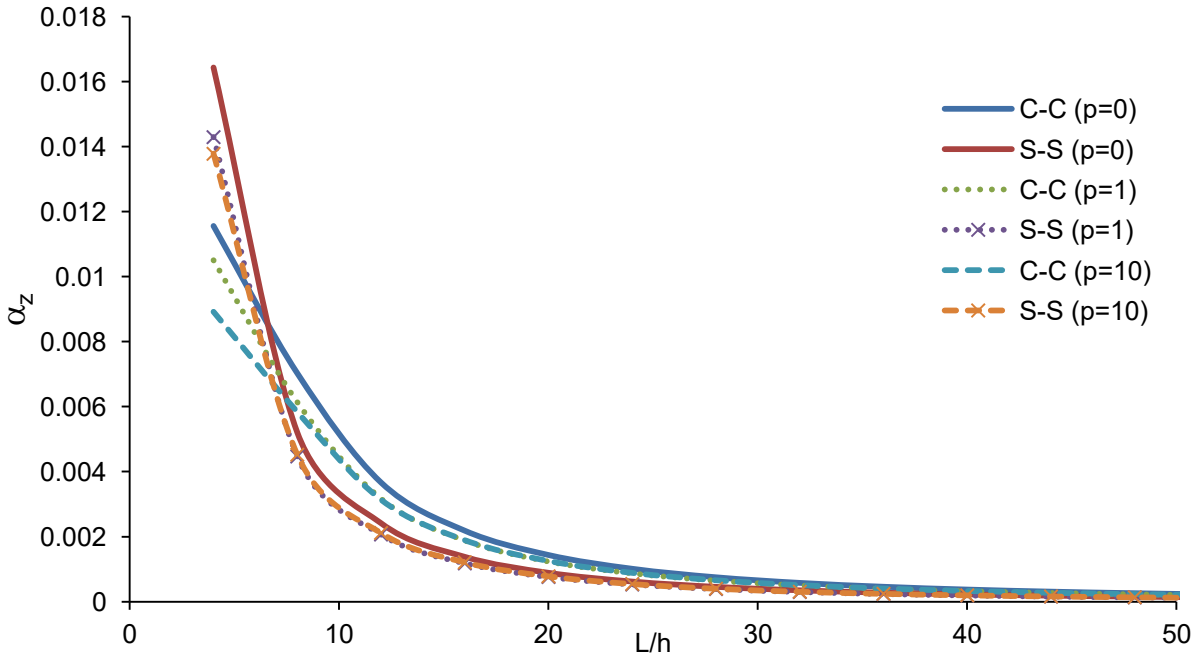

b. Thickness stretching parameter.

Figure 6: Variation of the shear deformation and thickness stretching parameters with respect to the slenderness ratio of FG beams (Type A, L/h=5 and 20).

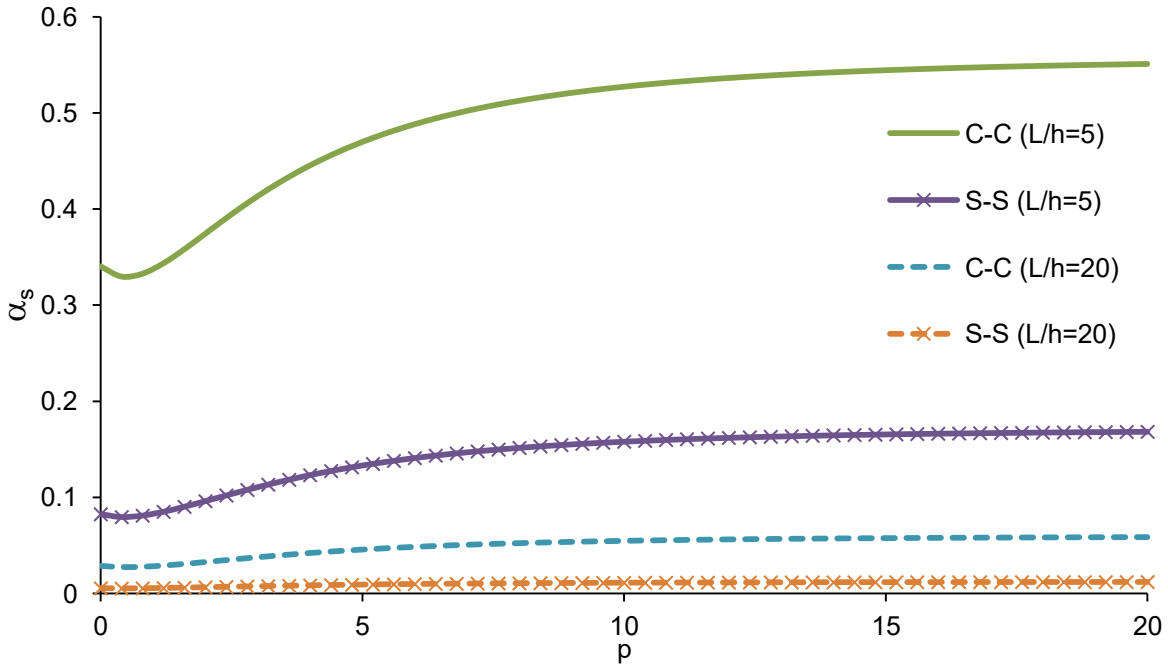

a. Shear deformation parameter.

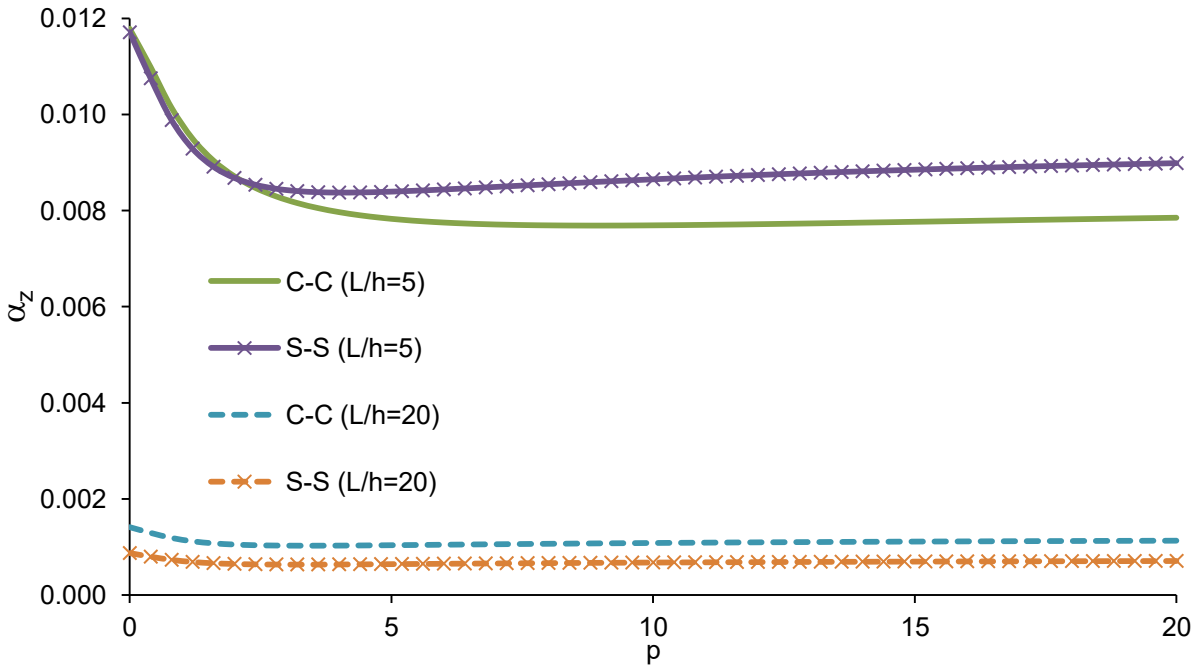

b. Thickness stretching parameter.

Figure 7: Variation of the shear deformation and thickness stretching parameters with respect to the power-law index of (1-8-1) FG sandwich beams (Type B, L/h=5 and 20).

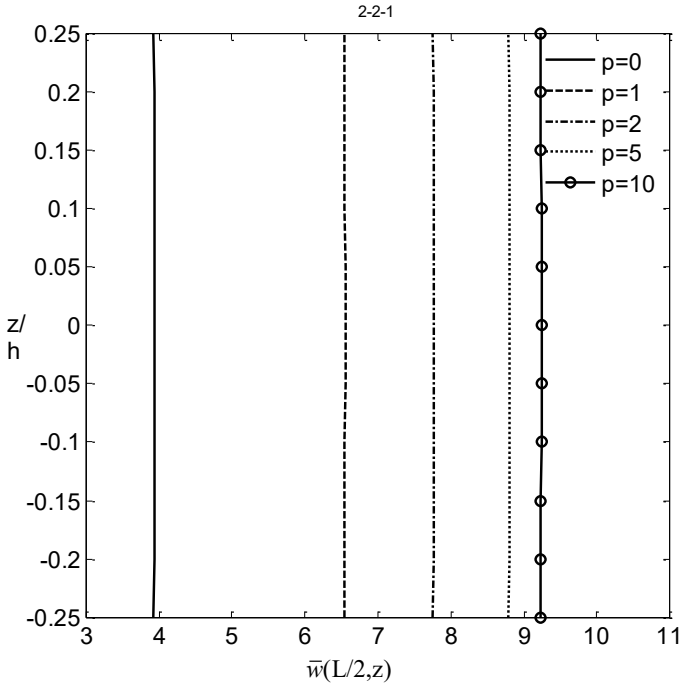

Figure 8: Variation of the vertical displacement through the thickness of (1-8-1) FG sandwich S-S beams under uniform load (Type B, L/h=5).

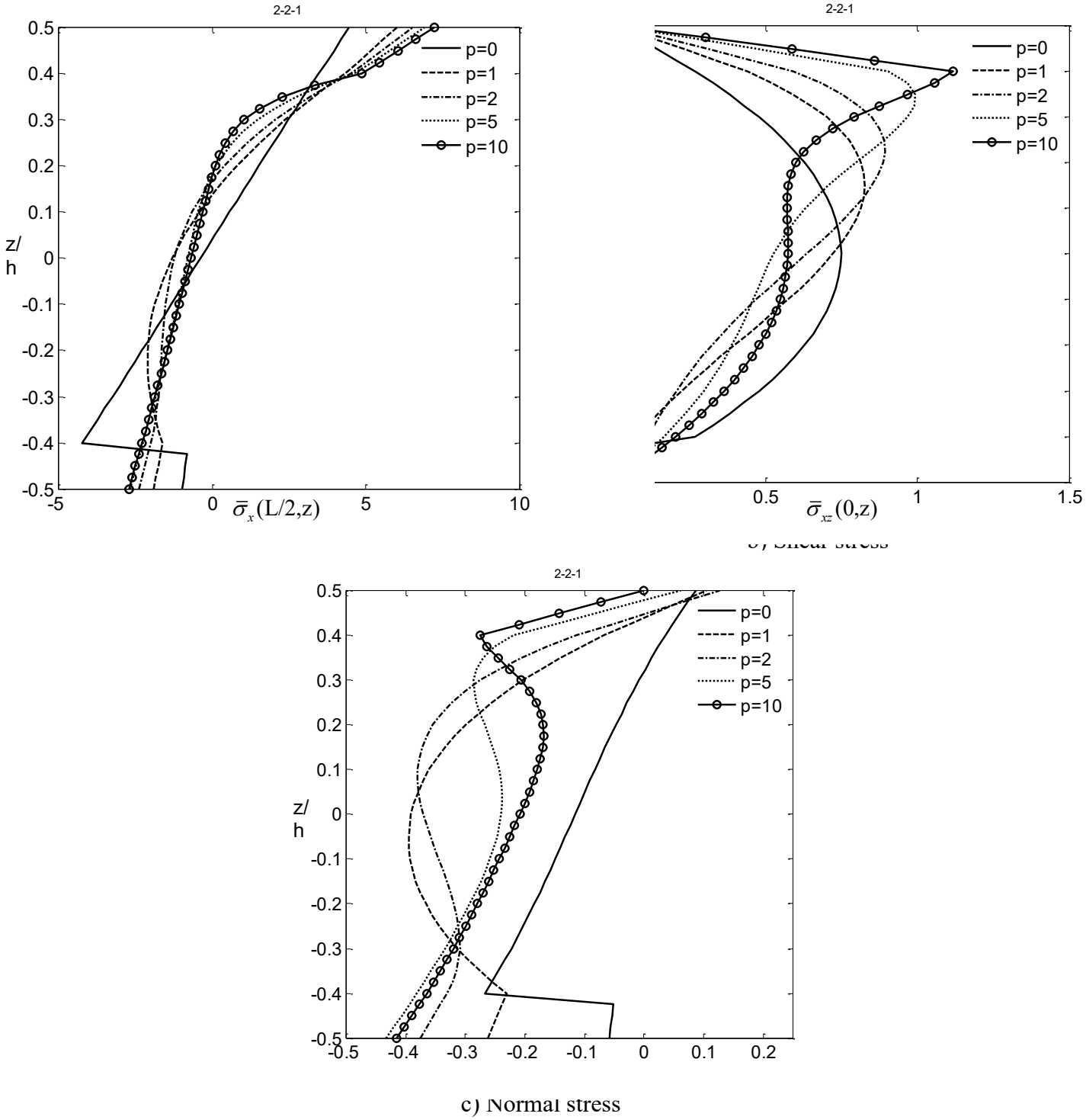

c) Normal stress

Figure 9: Variation of the stresses through the thickness of (1-8-1) FG sandwich S-S beams under uniform load (Type B, L/h=5).

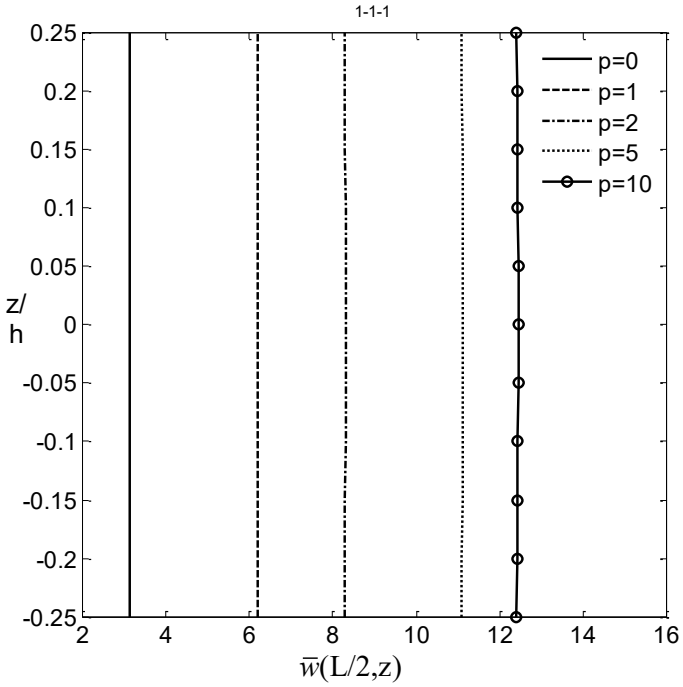

a) Symmetric scheme (1-1-1)

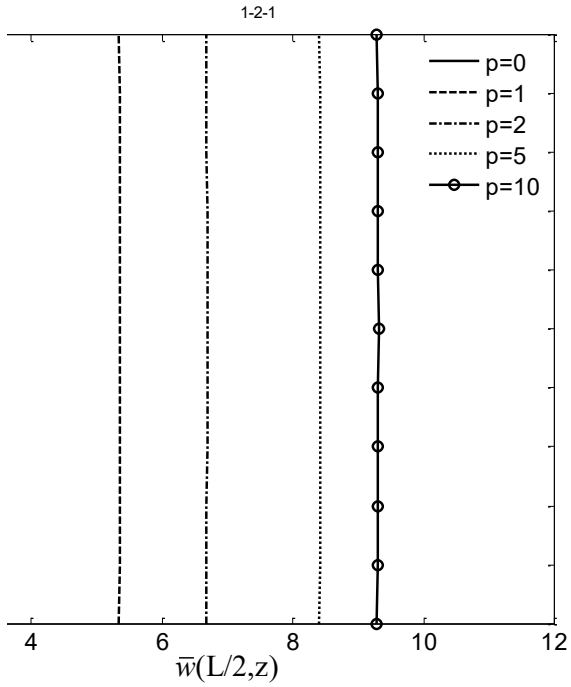

b) Symmetric scheme (1-2-1)

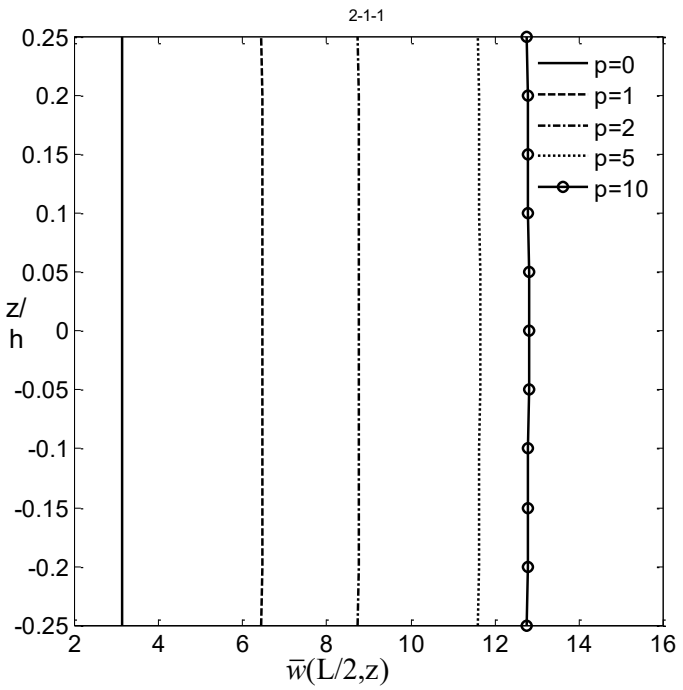

c) Non-symmetric scheme (2-1-1)

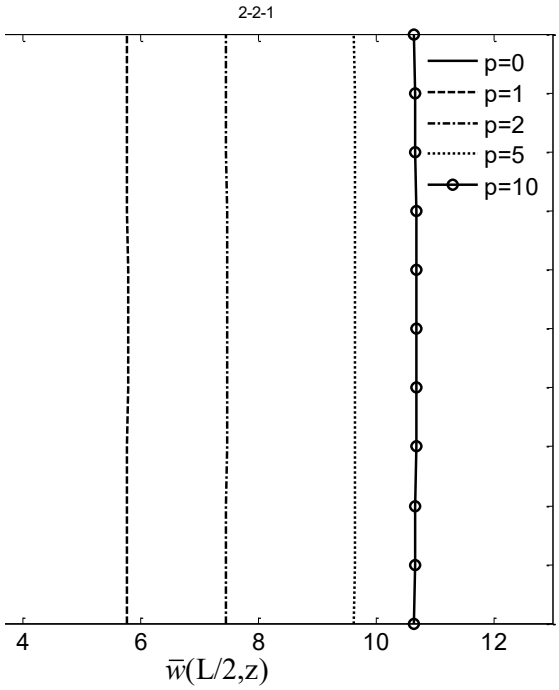

d) Non-symmetric scheme (2-2-1)

Figure 10: Variation of the vertical displacement through the thickness of FG sandwich S-S beams under uniform load (Type C, L/h=5).

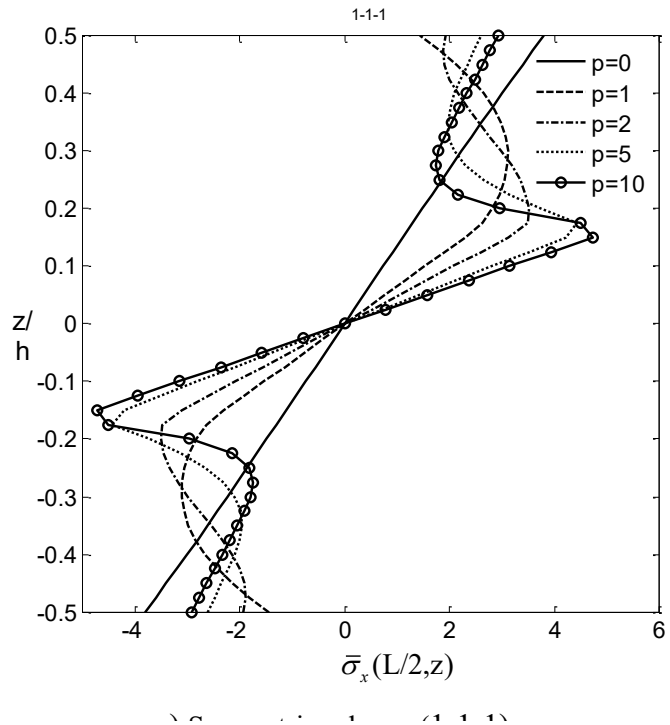

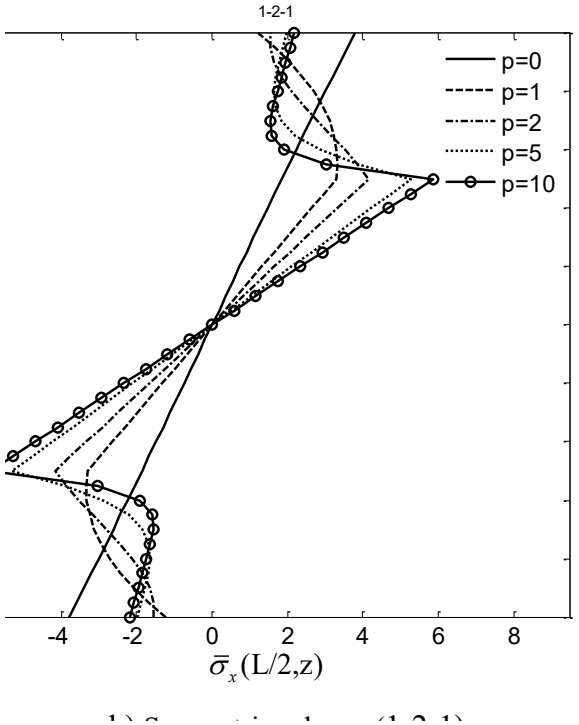

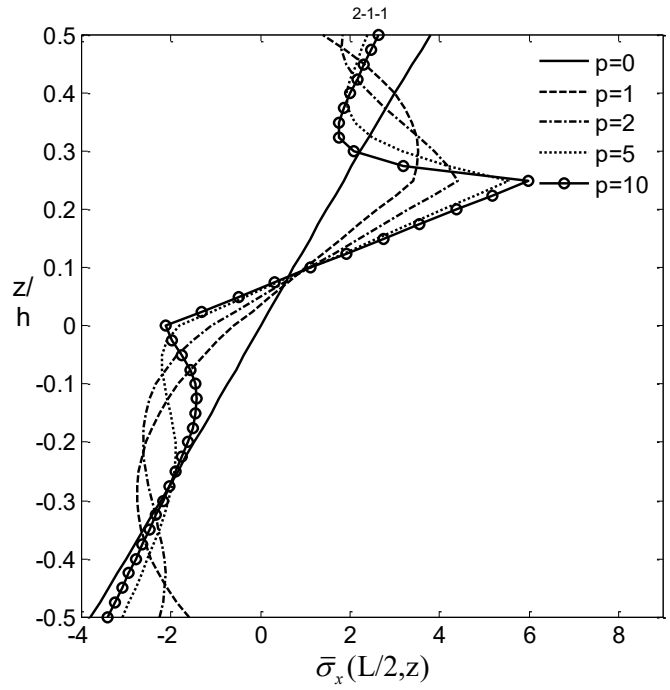

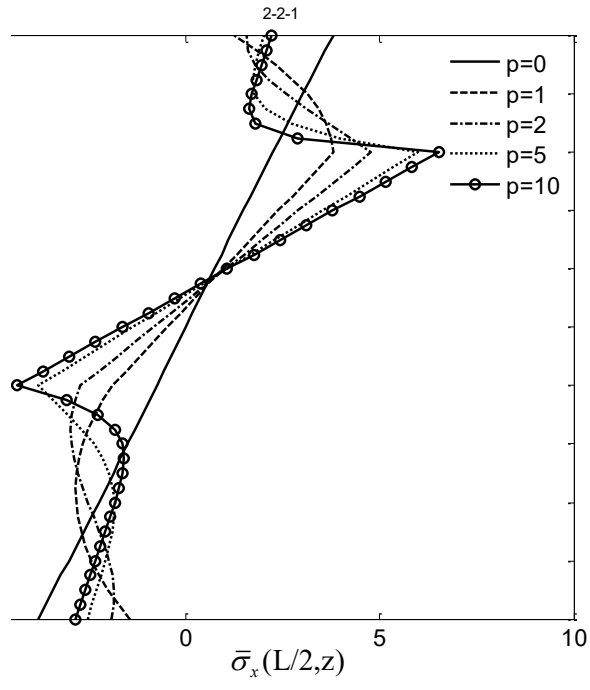

c) Non-symmetric scheme (2-1-1)

d) Non-symmetric scheme (2-2-1)

Figure 11: Variation of the axial stress through the thickness of FG sandwich S-S beams under uniform load (Type C, L/h=5).

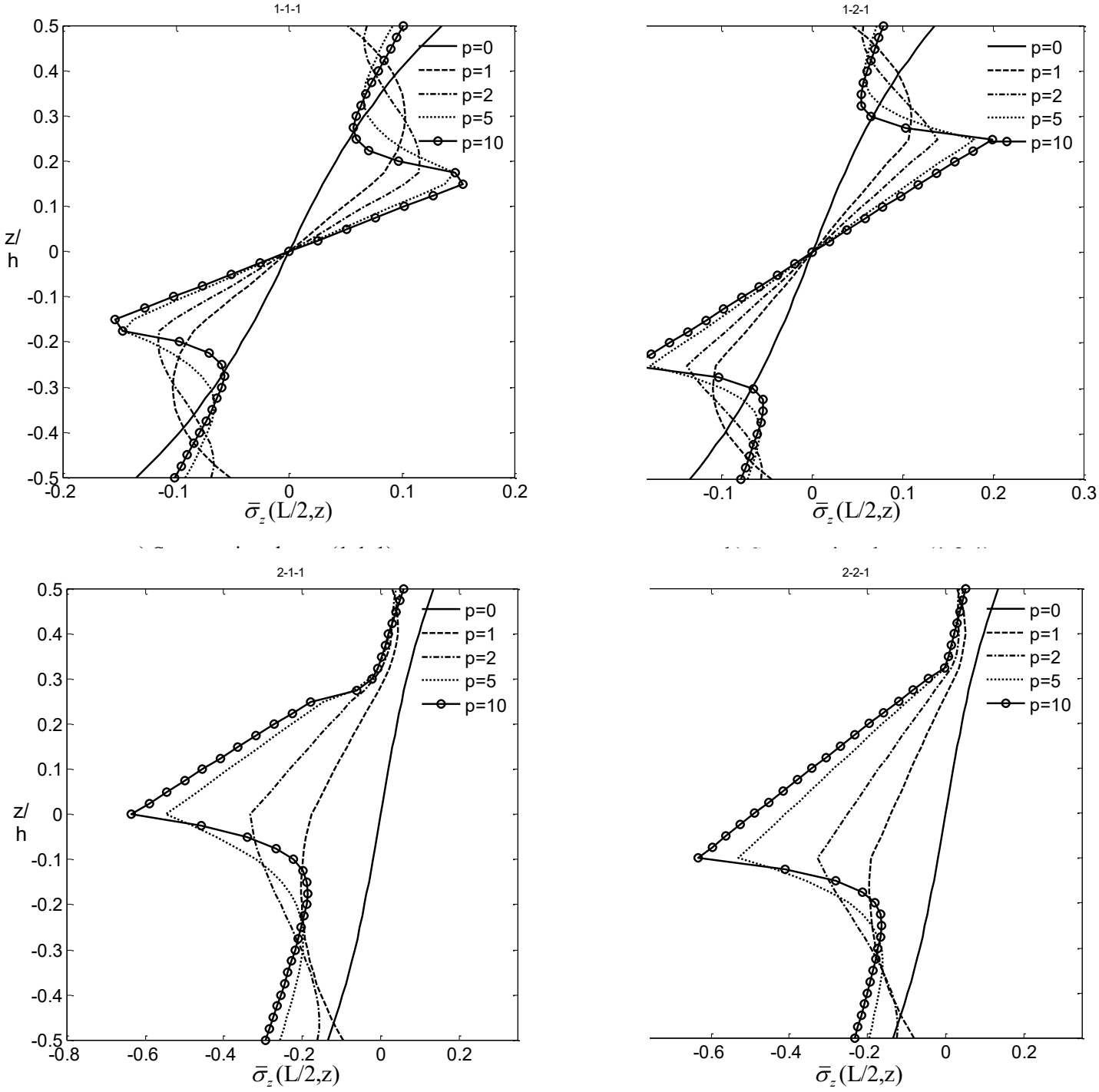

c) Non-symmetric scheme (2-1-1)

d) Non-symmetric scheme (2-2-1)

Figure 12: Variation of the normal stress through the thickness of FG sandwich S-S beams under uniform load (Type C, L/h=5).

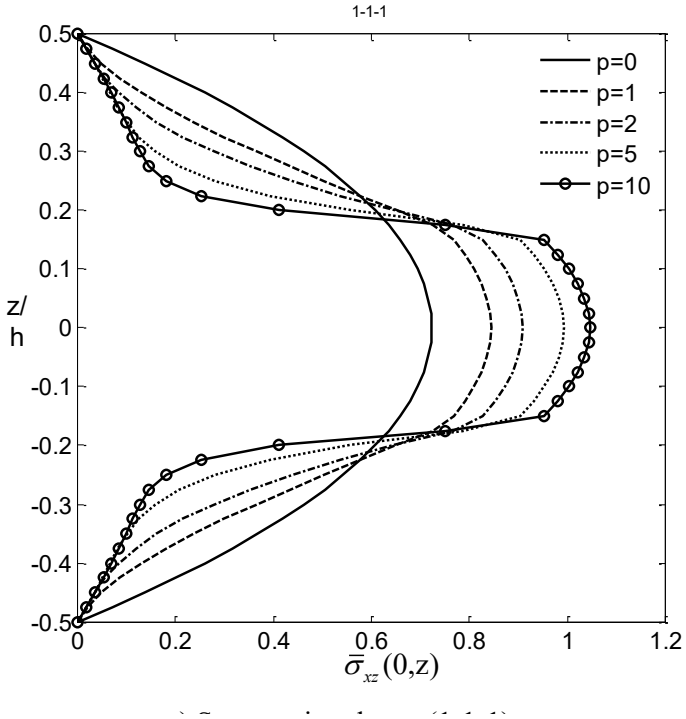

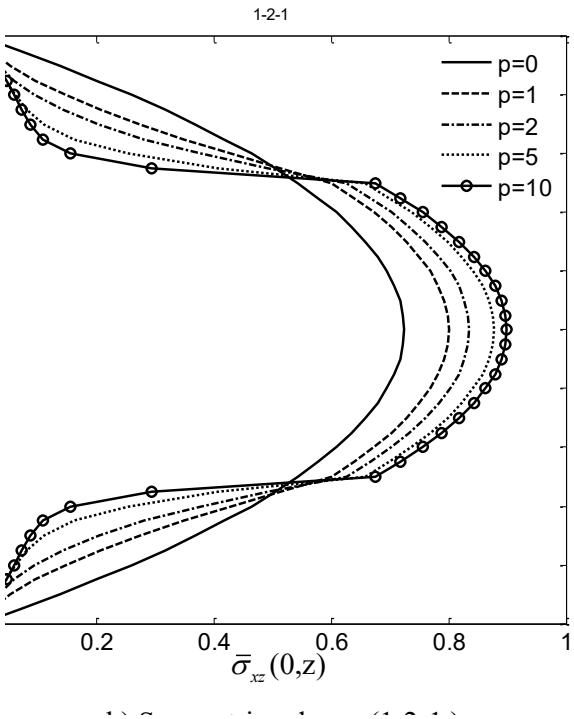

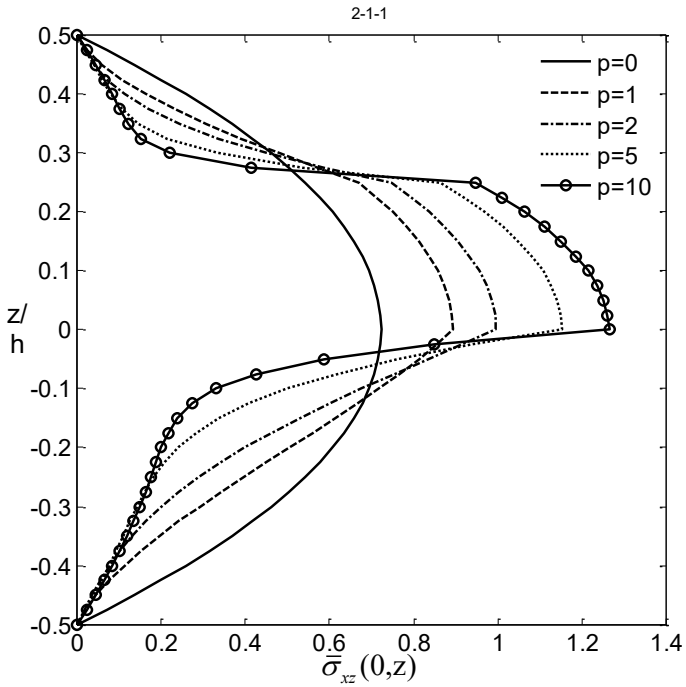

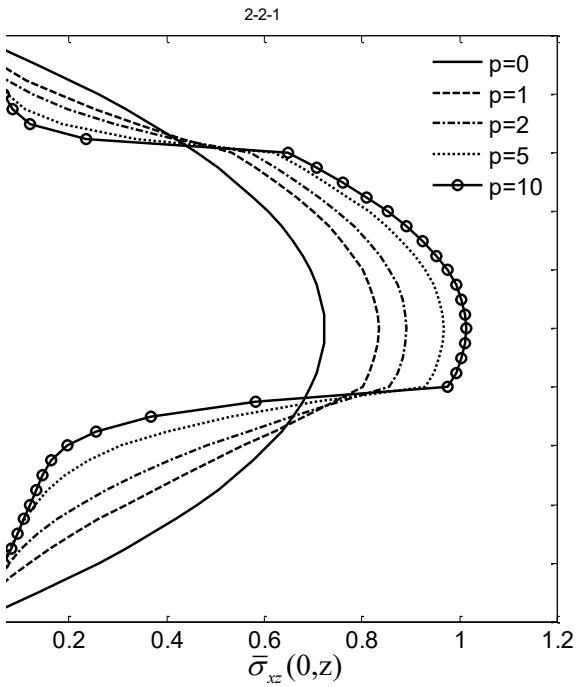

c) Non-symmetric scheme (2-1-1) d) Non-symmetric scheme (2-2-1)

Figure 13: Variation of the shear stress through the thickness of FG sandwich S-S beams under uniform load (Type C, L/h=5).